NASA TECHNICAL NOTE

NASA TN D-7218

NASA TN D-7218



# APPLICATION OF SONIC-BOOM MINIMIZATION CONCEPTS IN SUPERSONIC TRANSPORT DESIGN

*by Harry W. Carlson, Raymond L. Barger, and Robert J. Mack*

*Langley Research Center*
*Hampton, Va. 23665*

NATIONAL AERONAUTICS AND SPACE ADMINISTRATION • WASHINGTON, D. C. • JUNE 1973

# APPLICATION OF SONIC-BOOM MINIMIZATION CONCEPTS IN SUPERSONIC TRANSPORT DESIGN

By Harry W. Carlson, Raymond L. Barger, and Robert J. Mack
Langley Research Center

## SUMMARY

A study has been made of the applicability of sonic-boom minimization concepts in the design of large (234 passenger) supersonic transport (SST) airplanes capable of a 2500-nautical-mile range at a cruise Mach number of 2.7. Aerodynamics, weight and balance, and mission performance, as well as sonic-boom factors, have been taken into account. The results indicate that shock-strength nominal values of somewhat less than 48 newtons/meter$^2$ (1 pound force/foot$^2$) during cruise are within the realm of possibility. Because many of the design features are in direct contradiction to presently accepted design practices, further study by qualified airplane design teams is required to ascertain sonic-boom shock-strength levels actually attainable for practical supersonic transports.

## INTRODUCTION

No single factor is expected to exert a greater influence on the development of a worldwide high-speed air transport system than that of the sonic boom. Estimates indicate that a solution to the sonic-boom problem would more than double the potential supersonic transport market. The purpose of this paper is to review the present state of technology applicable to sonic-boom minimization and to provide a preliminary estimate of the extent of sonic-boom improvements that may result from application of these design concepts.

This study is based to a large extent on experimentally verified minimization concepts and computational techniques developed at the Langley Research Center during the height of activity in the national supersonic transport development program in the middle 1960's. At that time near-field minimization concepts were believed to offer promise for significant sonic-boom reduction in the transonic acceleration and supersonic climb portion of the flight but not for the supersonic cruise portion. Recent developments, however, warrant a reexamination of the situation. One of these is the introduction of refined minimization theory by George, Seebass, Jones, Barger and others. Another is the development, by Hayes, of a more accurate method of calculating sonic-boom propagation in a stratified atmosphere, which indicates a greater extent of airplane near-field regions than

previously believed. Finally, there is the advocacy of an airplane design philosophy, most effectively presented by Ferri, in which sonic-boom considerations play a dominant role. The greater part of the potential improvements may be associated with this latter approach, the "sonic boom configured" airplane.

In the present investigation four SST design concepts have been studied, two of which may be considered to be conventional approaches with only modest modifications for sonic-boom benefits, and two others which depart from conventional practices in accordance with the dictates of sonic-boom minimization concepts. In order to provide a realistic first estimate of the applicability of these concepts, the analysis accounts for the influence of airplane configuration on aerodynamics, weight and balance, and performance. Nominal ground track signatures are calculated at the begin-cruise point at a Mach number of 2.7 for supersonic transport designs estimated to have a performance capability for a 2500-nautical-mile range. The sensitivity of sonic-boom characteristics to selected design parameters is explored.

## SYMBOLS

Values are given in both SI and U.S. Customary Units. The measurements and calculations were made in the U.S. Customary Units.

| | |
|---|---|
| a | speed of sound, meters/second (feet/second) |
| b | wing span, meters (feet) |
| c | wing chord, meters (feet) |
| $\bar{c}$ | mean aerodynamic chord, meters (feet) |
| $C_L$ | lift coefficient |
| $C_D$ | drag coefficient |
| $C_m$ | moment coefficient |
| $F(\tau)$ | Whitham F-function |
| h | altitude, kilometers (feet) |
| L/D | lift-drag ratio |

| | |
|---|---|
| $M$ | Mach number |
| $\Delta p$ | overpressure, newtons/meter$^2$ (pounds force/foot$^2$) |
| $\Delta p_s$ | shock strength, newtons/meter$^2$ (pounds force/foot$^2$) |
| $t$ | signature duration, seconds |
| $W_c$ | airplane begin-cruise weight, kilograms (pounds mass) |
| $W_e$ | airplane empty weight, kilograms (pounds mass) |
| $W_g$ | airplane design gross weight, kilograms (pounds mass) |
| $W_1, W_2, \ldots, W_9$ | airplane weights at various phases of mission, kilograms (pounds mass) (see fig. 4) |
| x,y,z | directions along X-, Y-, and Z-axis, respectively; Cartesian coordinates |
| $\Gamma$ | wing dihedral angle, degrees |
| $\delta_c$ | canard deflection angle, degrees |
| $\delta_r$ | reflex-surface deflection angle, degrees |
| $\delta_T$ | horizontal-tail deflection angle, degrees |
| $\Delta$ | increment |
| $\tau$ | nondimensionalized length along X-axis used in Whitham F-function |

Subscripts:

| | |
|---|---|
| cg | center of gravity |
| LE | leading edge |
| max | maximum |

sub subsonic

sup supersonic

## THEORETICAL CONSIDERATIONS

### Signature Calculation

The calculation of airplane sonic-boom pressure fields is based on concepts arising from the linearized theory of supersonic flow. Area rule concepts are employed in the representation of the airplane as a particular body of revolution for a given set of flight conditions, and corrected linearized theory methods are used to define the body-of-revolution flow field. The process, which is described in some detail in references 1 and 2, is briefly reviewed in the following paragraphs.

Fundamental relationships, which permit a complete flow-field definition for bodies of revolution in a uniform atmosphere, were first formulated by Whitham (refs. 3 and 4). The key element of the Whitham solution is the F-function, which relates the form of the pressure signature near the body (but not too near) to the body shape. Subsequent operations performed on the F-function determine pressure signatures, including pressure jumps or shocks, for any desired propagation distance. The method of reference 5 developed by Hayes extends applicability of the techniques to a stratified atmosphere.

Definition of equivalent body-of-revolution geometry for lifting airplane configurations, such as those treated in the present study, requires consideration of both volume and lift contributions. Walkden's generalizations (ref. 6) of the Whitham theory and supersonic area rule considerations (ref. 7) permit definition of an equivalent area distribution due to lift and an area distribution formed by the airplane volume which are combined directly to yield an effective area distribution for the complete lifting airplane configuration. The equivalent area distribution due to lift is proportional to the cumulative lift of the configuration and in many cases, especially for supersonic transports, is found to be the dominant factor. Both area contributions are defined by the intersection of the airplane with supersonic area rule cutting planes tangent to the Mach cone and oriented azimuthally so that disturbances propagating normal to the planes are those which eventually reach the observer. When attention is confined to the airplane ground track, as in this study, a single equivalent body area distribution and a single F-function may be used to represent a given set of flight conditions (Mach number, weight, and altitude).

Figure 1 illustrates in general terms the procedure for computing a pressure signature from a given effective area distribution. First, the F-function, which represents the shape characteristics of the pressure signature, is evaluated from the area distribution by application of equation (14) of reference 3. The numerical implementation of this

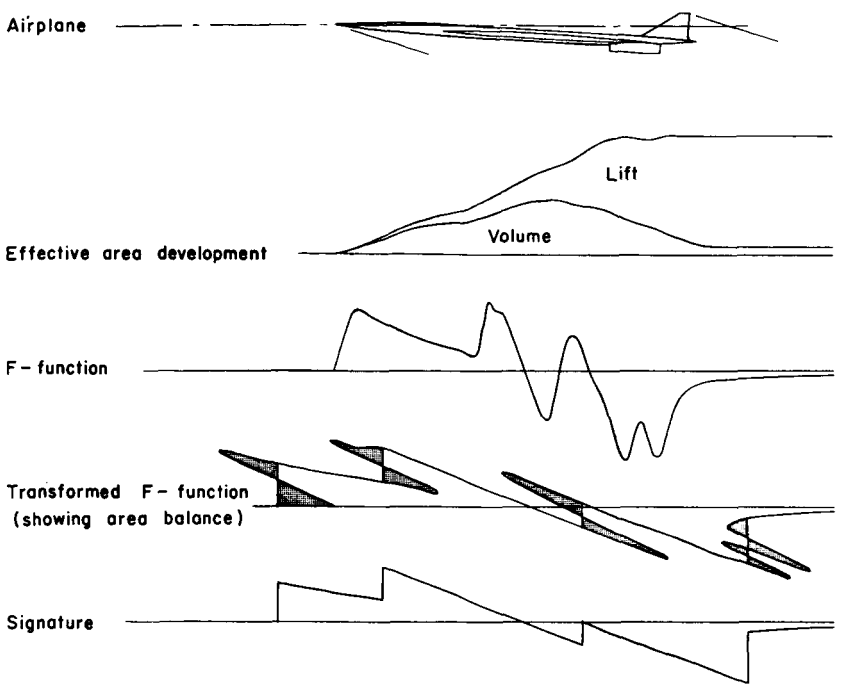


Figure 1.- Illustration of procedure for pressure-signature computation.

step employed in the present study is described in reference 8. Then, a transformed or distorted F-function, which accounts for signature shape changes in propagation through a stratified atmosphere, is computed according to the method of reference 5. Finally, multiple values of the resulting curve are eliminated by inserting shock discontinuities according to area balancing techniques, and a factor dependent on Mach number and propagation distance is used to convert F-function values to overpressures. Numerical means of performing the area balance and shock-location procedure for computer implementation are described in reference 9.

## Minimization Concepts

For cruising conditions of all supersonic airplanes flying today (including the Concorde), pressure signatures normally attain the far-field N-wave form at ground level. Minimization concepts for airplanes producing N waves presented in reference 10 have been found to offer little practical benefit because of drag penalties associated with the required shape changes (ref. 11). However, as pointed out in reference 12, for a sufficiently long and properly shaped airplane the pressure wave may develop so gradually that it does not attain the usual N-wave form by the time it reaches the ground. The dependence of signature shape on airplane shape in the near field was noted to offer significantly expanded opportunities for sonic-boom minimization. In references 12 to 14 F-functions and airplane effective area developments corresponding to certain types of presumably

desirable pressure signatures were examined. The greatest attention was given to a 3/2-power area development, which yields a plateau or flat-topped pressure signature. Wind-tunnel experimental studies of pressure signatures for bodies of revolution and airplane configurations employing that type of effective area distribution are reported in references 15 and 16.

Near-field minimization concepts became of even greater significance as a result of the Hayes analysis, which showed that a wave develops more gradually in the actual nonuniform atmosphere than it does in a uniform atmosphere. Moreover, the development becomes more and more gradual until it eventually stops (the wave becomes frozen in form), although the overpressure and impulse continue to decrease because of spreading.

Minimization concepts may also make use of the fact that when a signature with shocks is prescribed, those characteristic lines considered to be absorbed in the shock are not uniquely related to a given F-function. Therefore, as shown in reference 17, a certain part of the F-function can be arbitrarily specified, provided that the area-balancing condition is met and that multiple values of the F-function are avoided. To illustrate the point, figure 2 shows two F-functions that result in flat-topped signatures with identical shock strengths. One F-function has a constant-value positive section, and the other has an initial peak followed by a constant-value section. The first type of F-function corresponds to a 3/2-power area distribution included in the theoretical studies of reference 12. The second type of F-function allows an identical shock strength for an effective area

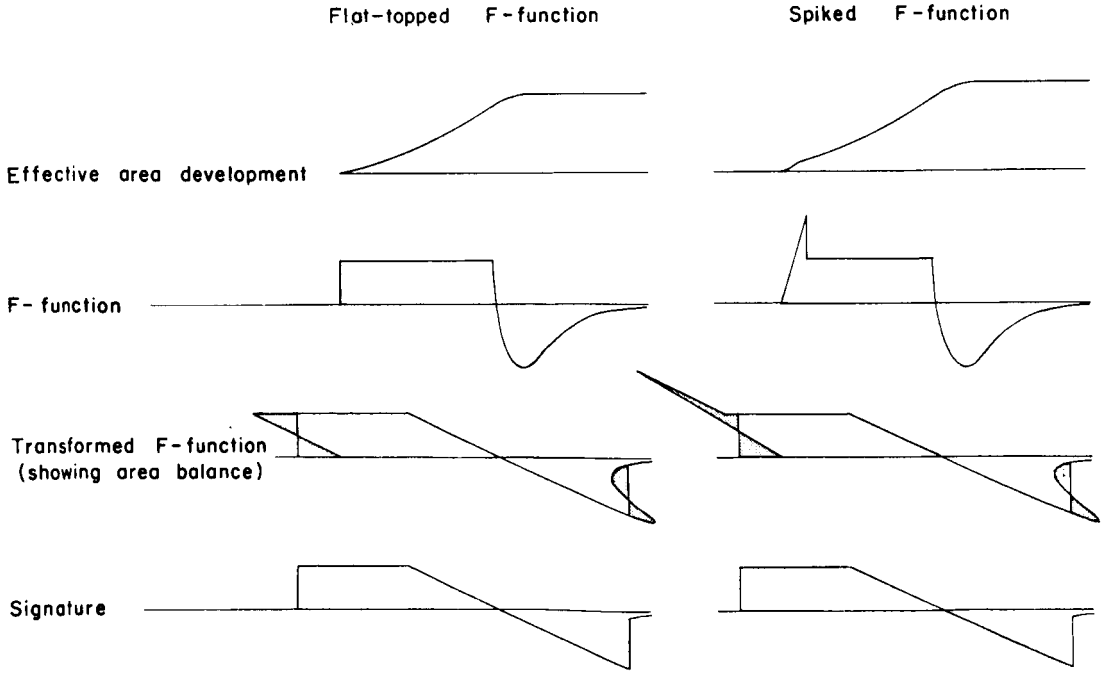


Figure 2.- Illustration of minimization concepts applied in present study.

development of the same length but of greater magnitude. In more practical terms, such a modification allows a smaller overpressure for comparable airplane size, weight, and operating conditions.

This question of determining what type of F-functions and area developments are preferable for sonic-boom minimization was treated initially by Jones (ref. 10). Jones demonstrated that the mathematical relationships are such that F-function ordinates near the origin are weighted more heavily in computation of the corresponding area development. Consequently, the resultant area under the F-function is reduced as equivalent bodies of a given maximum area are made more blunt, that is, as the effective area is crowded forward toward the origin. This principle has been utilized in the design of bodies to produce specified pressure signatures in both the near and far fields (refs. 17 and 18) and in the definition of lower bound signatures of certain classes (refs. 10, 19, 20, 21, and 22).

All the optimal F-functions given in reference 22, which summarizes minimization approaches, have a delta function at the origin (except for finite-rise-time signatures). However, if F-functions are designed with a forward spike of finite width, it is possible to take advantage of the Jones principle of accumulating area under the F-function near the origin while still retaining a reasonably small nose angle so as to prevent an inordinate drag penalty.

## APPLICATION OF MINIMIZATION CONCEPTS

### Minimization Goals

A fundamental difficulty encountered in attacking the sonic-boom minimization problem is that there is no well-established set of nominal pressure signature characteristics which would commonly be accepted as a solution to the problem. Furthermore, little is known of the relative importance of the various signature parameters, such as peak overpressure, shock strength, impulse, rise time, and so forth. Thus the designer is offered a choice of approaches to sonic-boom minimization (see, for example, ref. 22) but is given little guidance in the proper selection.

Shock strength is believed to be the controlling factor for outdoor annoyance; but for the far more common indoor exposure situation, noise and annoyance may be related to signature impulse and duration and other factors as well (ref. 23). For structural response and building damage criteria, the problem is equally complex (ref. 24).

Goal signatures for the present study have been taken to be of the plateau or flat-topped variety. Peak overpressure is thus the driving factor. Signatures of this type also offer a near-minimum impulse while requiring an airplane effective area development more easily attainable than that for a complete impulse minimization. Finite-rise-

time signatures (zero shock strength) were not considered because of the excessive length requirement. See references 25 to 27 for discussions of some rather exotic approaches for attainment of shockless signatures.

Configurations designed for sonic-boom minimization in this study were shaped to create an F-function with an initial spike. If properly prescribed, this spike allows a reduction in signature impulse and general overpressure levels. The F-function positive section following the spike was designed to provide a relatively smooth effective area distribution approximating that of a reasonable aerodynamic configuration. For the sonic-boom-designed configurations studied and for aerodynamically favorable cruise altitudes, this part of the F-function could often be made to be nearly constant. Somewhat lower values of shock strength are theoretically attainable if the F-function following the spike is allowed to increase; however, the required effective area distribution does not appear to be quite so compatible with good aerodynamic design. No attempt was made to minimize the tail shock by using the optimal F-functions, with a tail spike, given in references 21 and 22, because the complexity of airplane geometry in the aft region is such that a precisely prescribed area distribution of that type is virtually impossible to match. The method actually used was to make the approach to peak values in the aft region of the effective area distribution as gradual as possible. This approach reduces the tail shock jump in such a way that the signature is not sensitive to small variations in the area distribution. The actual calculation method proceeded as follows. By use of methods described in reference 17, idealized area distributions were computed from F-functions designed to yield favorable sonic-boom characteristics for a specified airplane length, weight, and flight altitude. Comparison of these area distributions with those of conventional arrow- and delta-wing designs led to new configurations with effective area distributions that more nearly approximated the idealized distributions. In most cases modifications were also required in the design F-functions so as to match more closely the area distributions of the actual configurations, which were determined from an analysis of aerodynamics, weight and balance, and performance characteristics. In some cases subsequent alterations of the configuration (such as a change in canard location, wing camber surface, or fuselage shape) were made to overcome a significant deviation from the idealized distribution. By this procedure the actual configuration area distribution and the sonic-boom-designed distribution were brought into close enough agreement so that the difference appeared to be resolvable through fine tuning.

## Design Parameters

When airplane design parameters such as Mach number, range, payload, size, weight, and cruise altitude have been set, application of sonic-boom minimization concepts may be carried out in a relatively straightforward manner. However, selection of these design parameters in such a way as to result in a complete optimization of sonic-

boom characteristics presents a complex problem involving a multitude of engineering disciplines. Charts of sonic-boom signature characteristics as a function of individual design parameters are useful only if the full interrelationship of the parameters are known. For example, the variation of shock strength with Mach number for a certain class of optimized signatures may be defined with all other design parameters being held constant. This, however, is not realistic because the optimum cruise altitude varies with Mach number, and the airplane weight for a specified mission certainly does not remain constant. Only if all these interrelationships are accurately known can a complete optimization process be carried out. Such a complete process is beyond the scope of the present study. Instead certain design parameters have been selected on the basis of what is believed to be reasonable from past experience, and the study is restricted to the application of minimization concepts for those conditions.

The choice of a cruise speed of $M = 2.7$ for this study is predicated on a number of considerations. As outlined in reference 28, aerodynamic and propulsion factors tend to optimize range and payload at speeds slightly lower than $M = 3$. At lower speeds and at the associated lower cruise altitudes, near-field sonic-boom characteristics are more pronounced and somewhat reduced shock strengths might be achieved, but at the expense of reduced airplane utilization and poorer economics. At higher speeds, the associated higher cruise altitude exerts a strong influence on shock-strength attenuation, and if sonic-boom characteristics were dictated by far-field relationships, the advantage would lie with the higher speed. However the potential gains associated with near-field sonic-boom design methods decrease rapidly with increased speed, and it is uncertain that any sonic-boom advantages would remain at speeds greater than that chosen. Furthermore, at higher speeds some very difficult materials problems arise, particularly in the non-metallics area (i.e., transparencies, tires, sealants, lubricants, etc.), that raise further questions of feasibility. Another reason for the speed selection is that to be really meaningful such a study must be based on reasonably accurate data from all engineering disciplines, and for the speed regime of $M = 2.7$, a significant body of such data does exist at the present time.

Design range for the study is 2500 nautical miles, which represents the coast-to-coast distance over the continental United States. This is believed to be a minimum useful range for a supersonic transport and is set in large part by the desire to achieve low values of sonic-boom overpressure. The influence of increased design range is treated in a subsequent section of this paper.

Payload has been selected as 21 000 kg (48 000 lbm) representing 234 passengers. Any substantial reduction in payload is not believed to be acceptable to the airlines because of the impact on economics. Furthermore, sonic-boom benefits associated with payload reduction might not be so sizable as might be imagined. Recall that very small

supersonic military airplanes carrying only one person produce overpressures of about 24 $N/m^2$ (0.5 $lbf/ft^2$) and that such airplanes are not amenable to near-field minimization redesign concepts. Possibly, because of the sonic-boom benefits of increased length, the advantage may lie in airplanes of greater passenger capacity.

For many years the airplane effective length has been known to be an extremely important consideration in sonic-boom minimization. Airplane configurations studied in great depth in the national supersonic transport program had fuselage lengths from about 85 meters (280 feet) to about 90 meters (295 feet). However from a sonic-boom standpoint, these designs failed to make effective use of the length. Although some slight increase in fuselage length has been allowed for the sonic-boom-dictated designs of this study, the primary emphasis has been on configuration modification to make more effective use of the lengths already being considered. Theoretical studies indicate that for the design conditions assumed, additional reductions of shock strength of about 25 percent could be realized with a 50-percent increase in effective length, provided that weight penalties are not incurred. Increased effective length might be achieved by a simple airplane stretchout or by use of vertically separated multiplane lifting surfaces. In either case, however, there are certain to be weight penalties that tend to counteract or even reverse the projected gains. Because of uncertainties in aerodynamic and weight estimates for configurations, which depart severely from conventional design practices, configurations studied herein were limited to those with less severe, but still appreciable, changes in design approaches.

Airplane weight is not an independent variable, but is determined by the choice of the previously discussed design parameters. In this study an attempt has been made to provide an assessment of the resultant weight for several sets of assumptions regarding projected technological advances. Cruise altitude is also considered as a variable, and an attempt is made to define an optimum altitude from a sonic-boom standpoint for the assumed design conditions.

## Study Methods

This study of the applicability of minimization concepts to the reduction of supersonic transport sonic boom in cruise takes into account aerodynamics, weight and balance, and mission performance, as well as sonic-boom factors. A pictorial outline given in figure 3 may help to explain the organization of the study elements now described.

Theoretical concepts for sonic-boom minimization, discussed previously, are employed in the definition of numerical models of SST configurations believed to offer significant shock-strength reduction. These geometric data are then used in a series of aerodynamic computer programs (refs. 29 and 30) for evaluation of cruise Mach number,

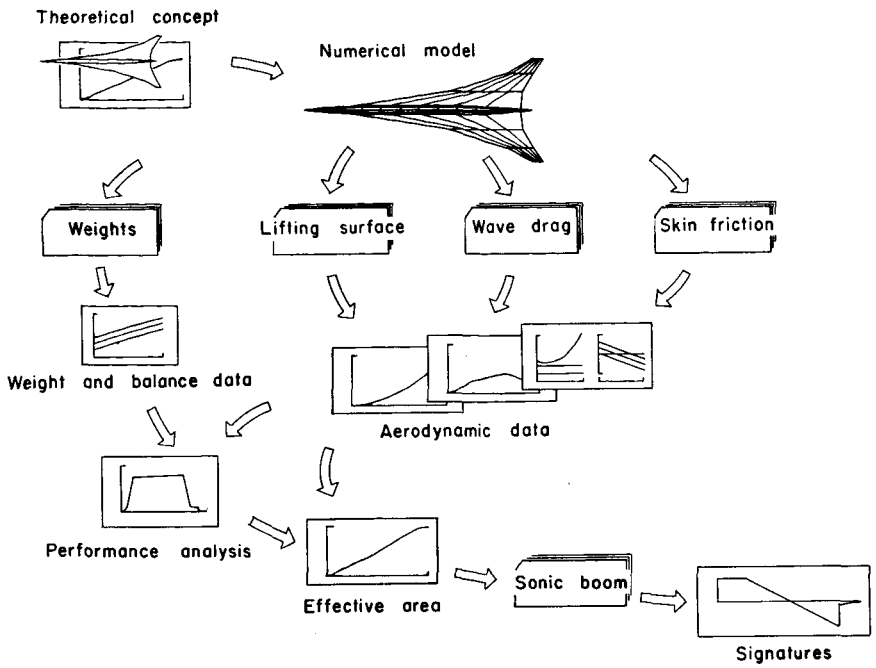


Figure 3.- Outline of method used to obtain sonic-boom pressure signatures.

lift, drag, and pitching moment and for evaluation of lift and area distributions. A computer program for the design of a minimum-drag twisted and cambered wing surface is also employed. As pointed out in references 29 and 30, these design and analysis methods have been found to be reasonably accurate for SST configurations, which generally meet the linearized theory requirements for thin wings and slender bodies.

Subsonic aerodynamic data are obtained from the same skin-friction computer program that is employed at supersonic speeds and from experimental drag-due-to-lift factors for thin delta wings of equivalent aspect ratio (ref. 31). No attempt was made to generate independent aerodynamic data for the transonic speed range. Up to $M = 1.0$, the lift-drag ratio of a configuration under study was assumed to bear the same relationship to the lift-drag ratio for the reference delta-wing configuration as at subsonic speeds. Beyond $M = 1.0$, the lift-drag ratio of a configuration under study was assumed to bear the same relationship to the lift-drag ratio for the reference delta-wing configuration as at the cruise Mach number.

Airplane weight and balance estimates are based on parameterized state-of-the-art data for current transport airplanes and for SST designs, which were studied in some depth in the national program. A computer program was employed in this phase of the work. Note that the weight estimates do not account for any unusual configuration-dependent problems that may be encountered in airplane development and that certain design factors such as aeroelasticity and flutter have not been addressed.

The aerodynamic and weight data serve as input information for a simplified performance analysis. For the purposes of this study, basic performance characteristics for a 2500-nautical-mile mission of a conventional delta-wing SST designed for a cruise Mach number of 2.7 were established and fuel consumption in the various mission segments for other vehicles was proportioned according to estimated trimmed lift-drag ratios. Figure 4 outlines the system employed and uses, as an example, the reference

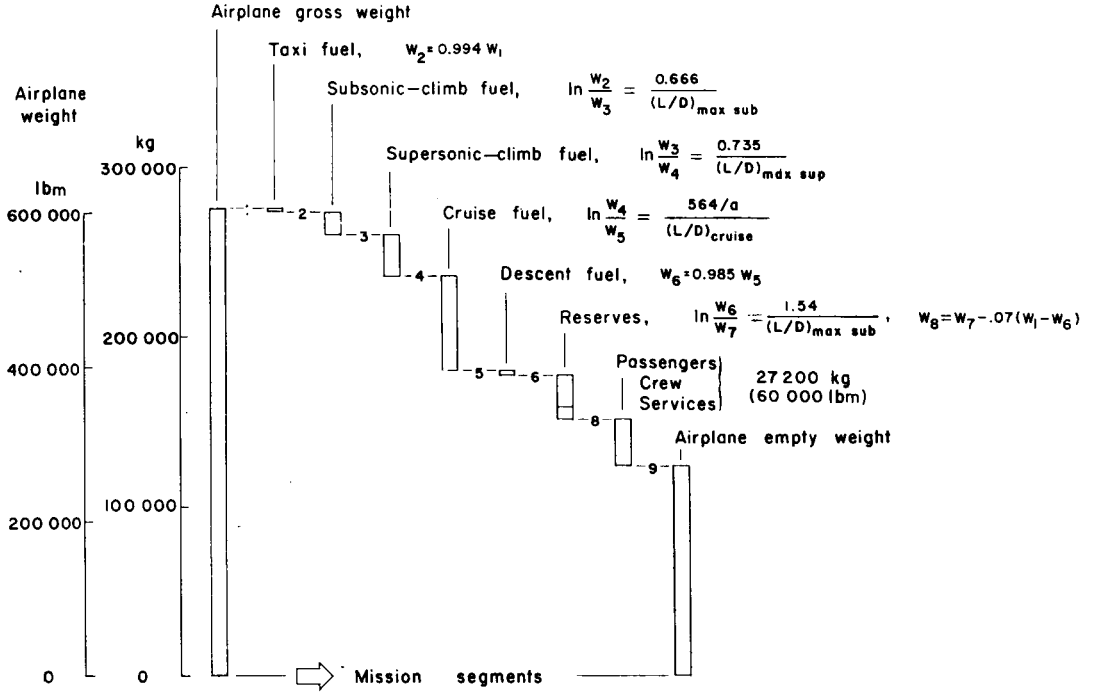


Figure 4.- Outline of simplified performance analysis. Example shown for reference delta-wing SST mission.

conventional delta-wing SST mission. The chart is generally self-explanatory. From a given assumed gross weight, fuel weight consumed in the mission segments is subtracted in a step-by-step procedure moving from left to right. The resulting empty weight is then compared with an estimate from the weight analysis for the given assumed gross weight, and by an iterative procedure or through graphical means a gross weight and fuel consumption schedule, which satisfies both the performance and weight analysis, is found. Subsequent examples may help to clarify the matching process.

From area and lift developments corresponding to begin-cruise conditions, the sonic-boom effective area is determined and the sonic-boom analysis methods previously described are used to predict nominal ground track signatures. For this purpose a single combined sonic-boom computing program is employed. It employs the method of reference 8 for F-function determination, the method of reference 7 for atmosphere propagation, and certain features of the method of reference 9 for automated determination of

shock location. A ground reflection factor of 1.9 is assumed for all signature calculations. If departures from the desired signature characteristics are found to be too large, incremental changes in the SST design and numerical model which restore the desired signature shape (but not necessarily its magnitude) may be defined, and the entire process may be repeated until a converged solution is found. In many cases, however, the required configuration changes are relatively small, and differences in aerodynamic and weight characteristics are within the accuracy bounds of the analysis systems. Thus, it can be assumed that the revised goal signature may be attained by design modifications (fine tuning), which do not appreciably affect the weight, and time-consuming iterations may be avoided.

Sonic-boom predictions for the climb and acceleration portion of the flight have not been made because the simplified performance analysis did not allow definition of a complete flight profile. Limitation of climb and acceleration sonic-boom parameters to values no greater than those for cruise might require departures from an assumed optimum performance flight path and result in somewhat greater airplane weight and somewhat higher sonic-boom levels.

## Airplane Configuration

A number of supersonic transport configurations, which depart rather drastically from conventional design practices so as to implement sonic-boom minimization concepts, have been advanced in references 32 and 33. The studies reported therein did not consider the impact of sonic-boom-dictated design features on aerodynamics, weights, performance, and so forth; thus, predicted sonic-boom characteristics could be considered as goals, but not as an indication of attainable values. The work, however, pointed out large potential improvements and emphasized the need for careful consideration of design concepts differing from conventional approaches according to the dictates of minimization theory. Some problems associated with implementation of sonic-boom considerations in practical airplane design are treated in reference 34. Configurations treated in the present study do not depart from conventional practices to the extent of the more imaginative designs of references 32 and 33; nevertheless they do offer quite substantial theoretical sonic-boom improvements and are subject to evaluation by use of current state-of-the-art methods.

Three-view drawings of the four basic SST design concepts considered in this study are presented in figure 5. The conventional delta-wing design is patterned closely after an airplane configuration that was studied in great depth in the national SST program and is herein taken as a reference or a baseline configuration. Subsonic aerodynamic performance factors exerted a large influence on the choice of the delta-wing planform, and as a result the supersonic leading edge of the major portion of the wing at the cruise Mach

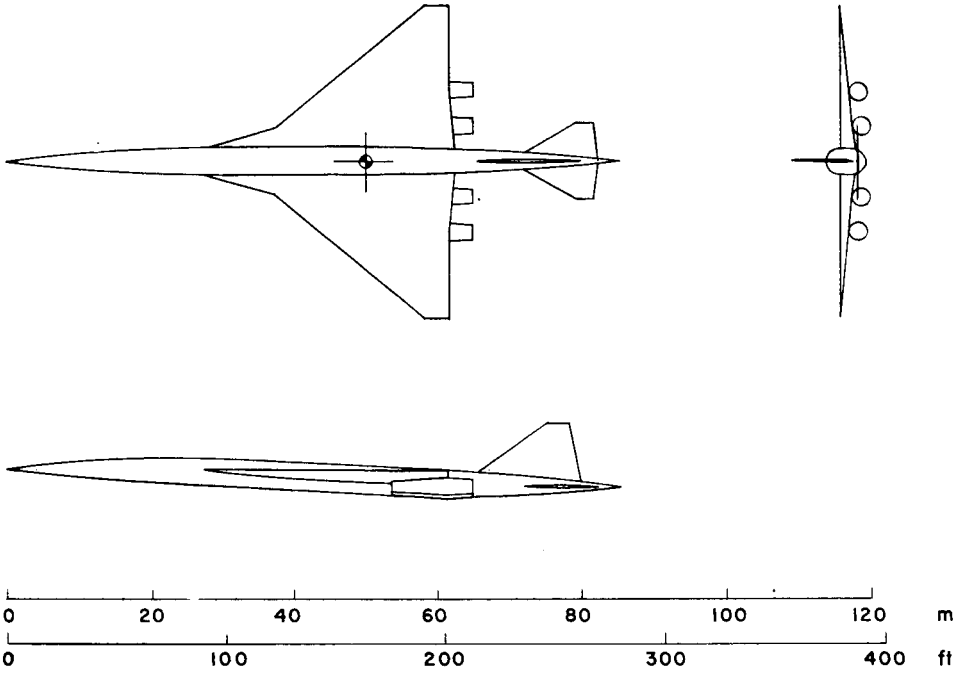


(a) Delta-wing configuration.

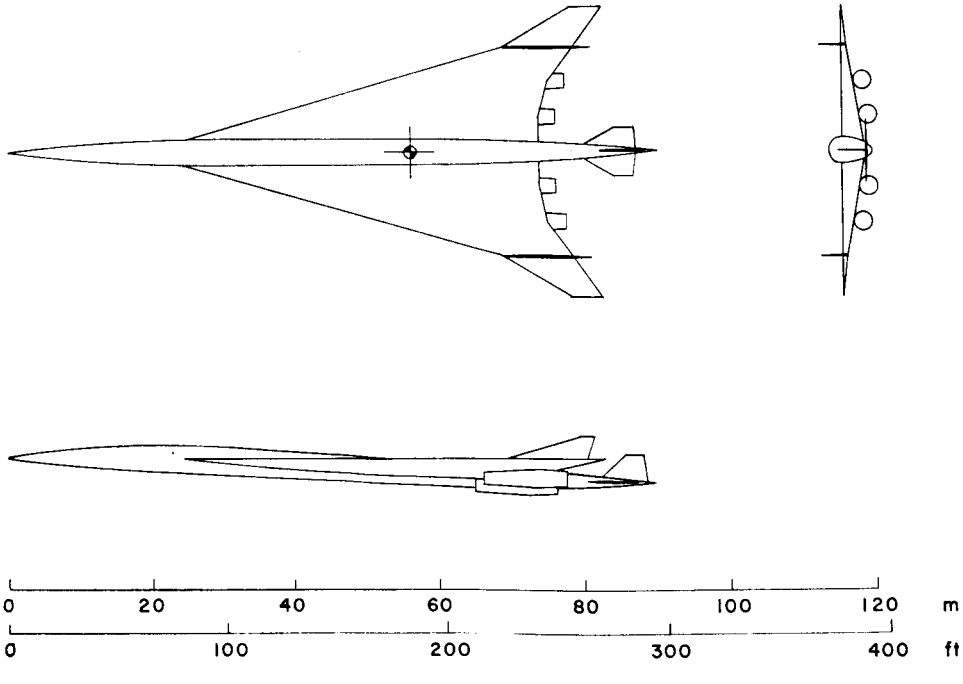


(b) Arrow-wing configuration.

Figure 5.- Basic SST designs in sonic-boom study.

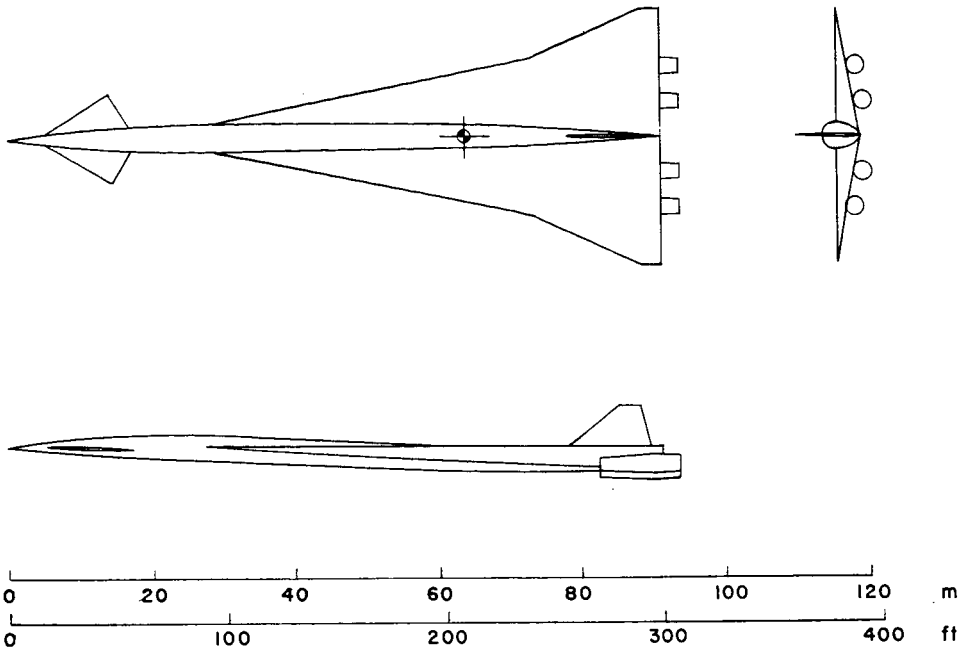


(c) Aft delta-wing configuration.

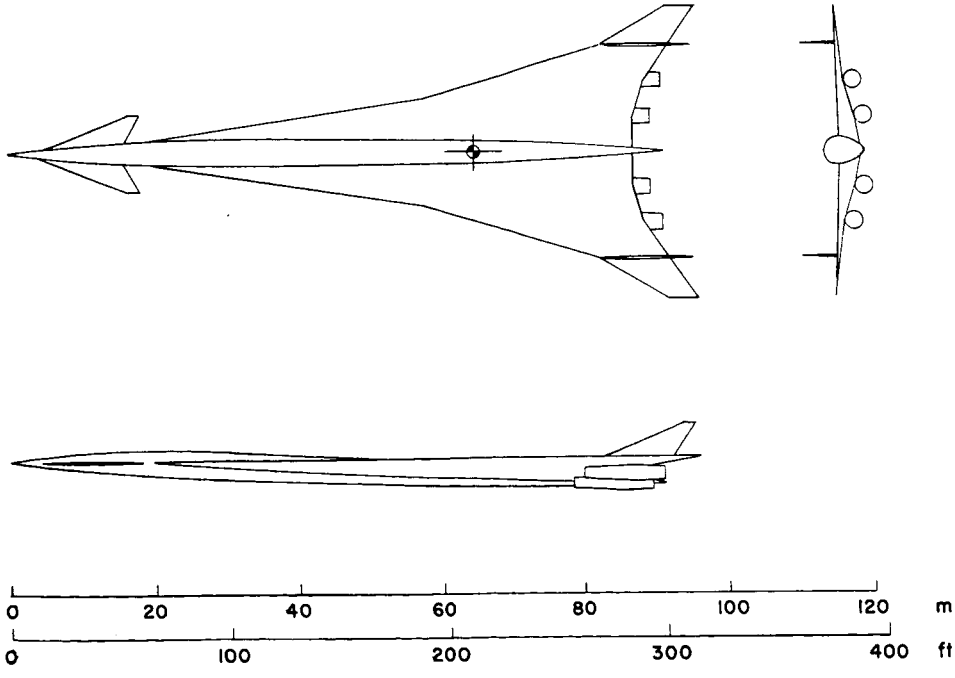


(d) Aft arrow-wing configuration.

Figure 5.- Concluded.

number of 2.7 is not conducive to attainment of a high degree of cruise aerodynamic efficiency nor low levels of sonic-boom overpressure. The conventional arrow-wing design, which offers improvements in cruise aerodynamic efficiency and sonic boom possibly at some expense in low-speed characteristics, has also been studied in some depth. In contrast, the remaining two design concepts are purely conceptual and are based primarily on sonic-boom minimization considerations discussed in the section of the paper entitled "Theoretical Considerations." The aft delta-wing design closely resembles a design approach presented in reference 32. The final design represents an attempt to combine good sonic-boom design practices with retention of the cruise aerodynamic efficiency afforded by an arrow wing.

Note that the designs based primarily on sonic-boom minimization considerations require relatively large wing areas. Long root chords are needed to provide the gradual development of area and lift dictated by sonic-boom design criteria; the span however cannot be decreased correspondingly because of the need to preserve aerodynamic lifting efficiency at both subsonic and supersonic speeds. Also note that these configurations designed specifically for sonic-boom benefits are characterized by a wing location well aft of that dictated by conventional design practices. One reason such aft wing arrangements are normally avoided is that the centroid of the wing volume available for fuel storage is placed at a long distance from the empty-weight center-of-gravity position. If the main portion of the available wing fuel-storage volume is to be used, the airplane balance problem is aggravated by large shifts in airplane center-of-gravity position and excessive trim drag is encountered. However, with the large wing area required in sonic-boom design, sufficient fuel-storage volume may be found in the forward portion of the wing so that the problem may not be severe, at least not for design ranges of 2500 nautical miles. The canard control surfaces of these designs, acting in combination with a slender fuselage, may aggravate aeroelasticity problems. These and other questions associated with departures from conventional design practices need to be explored but are beyond the scope of the present study.

A detailed geometric representation of the four SST design concepts depicted in figure 5 is given in tables 1 and 2. Table 1 presents a description of the numerical models used as input data for the wave drag computer program. Readers unfamiliar with the format of the tabular data may consult reference 35. For the wave drag analysis, the wing was considered to be at an angle of attack, but no account was taken of the wing twist and camber. Wing mean camber surfaces were however considered in other phases of the analysis, and ordinates are given in table 2. Some of the more pertinent geometric parameters are summarized in table 3.

## AERODYNAMIC ANALYSIS

Estimated aerodynamic characteristics for the four basic SST design concepts have been obtained through employment of analytic techniques discussed under the section entitled "Study Methods." Lift, drag, and moment characteristics for the cruise Mach number of 2.7 are shown in figure 6.

Cruise Mach number wave drag has been evaluated through use of supersonic area rule concepts implemented by a computing program described in reference 36. Skin-friction estimates were obtained from a computer method, which divides the airplane into streamwise strips, assigns to each a characteristic Reynolds number and skin-friction coefficient, and sums the resultant forces. In the study, whenever cruise altitude was varied from the base point value of 18.3 km (60 000 ft), account was taken of changes in skin-friction drag coefficient.

Wing camber surfaces were defined by a computing program (described in ref. 37), which optimizes the surface for a minimum drag at a given design lift coefficient. Because of loading distribution sensitivity, choice of the design lift coefficient was affected by trim and sonic-boom design considerations, as well as by the desire to obtain high values of maximum lift-drag ratios. The design surface was also modified to avoid extreme local slopes and to provide a more realistic shape for incorporation into a practical airplane. The resultant wing surfaces described in table 2 were employed in a computer program for the evaluation of aerodynamic characteristics of specified wing shapes. Basic principles of the program are set forth in reference 38. A specialized version of the method (ref. 39), which permits consideration of deflected control surfaces, was used in obtaining the drag-due-to-lift and moment data shown in figure 6. An account has been made of drag increments associated with control-surface deflections which provide a zero moment about the assumed airplane center of gravity; thus, the lift-drag polars presented may be considered to be trimmed. For the aft delta-wing and the aft arrow-wing configurations, control is to be provided by the canard surface. The cruise-point canard setting however is assumed to be selected on the basis of sonic-boom design considerations, and cruise-point trim is assumed to be provided by a selected but fixed deflection of a reflex area designated by the shading in the sketch.

It has been noted that, for the sonic-boom-controlled designs, increased drag due to lift results from the reduced wing aspect ratio, but this is compensated for by a reduced wave drag brought about primarily by the aft wing location.

Trimmed lift-drag polars were obtained only for the cruise Mach number. Other aerodynamic data for use in performance analysis were approximated in terms of departures from effective lift-drag ratios assigned to the several segments of the reference

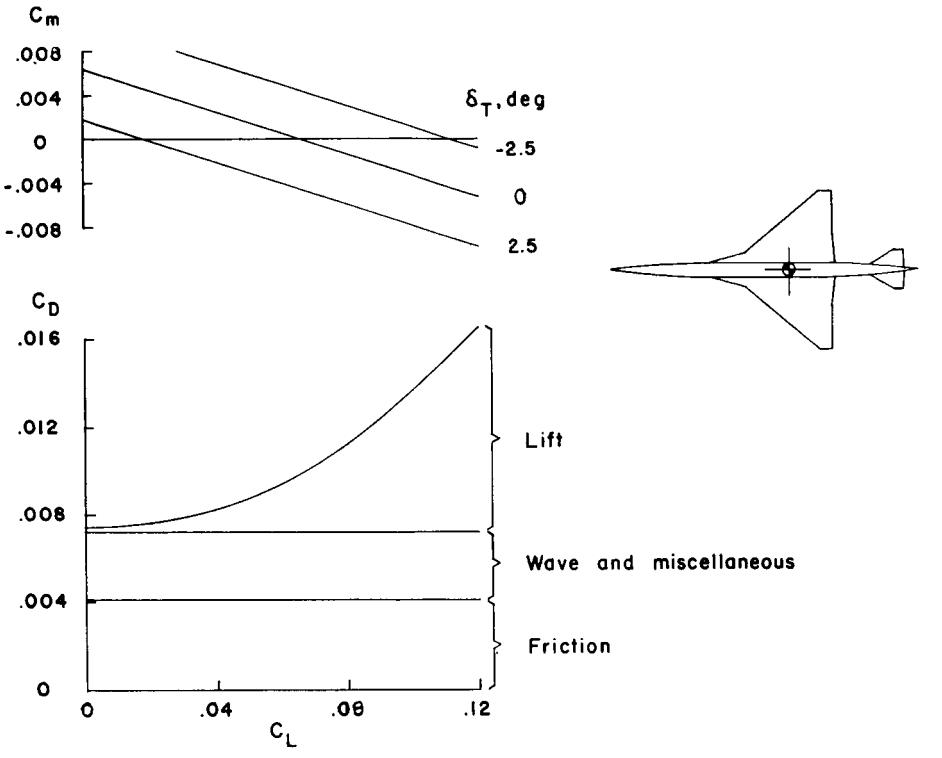


(a) Delta-wing configuration.

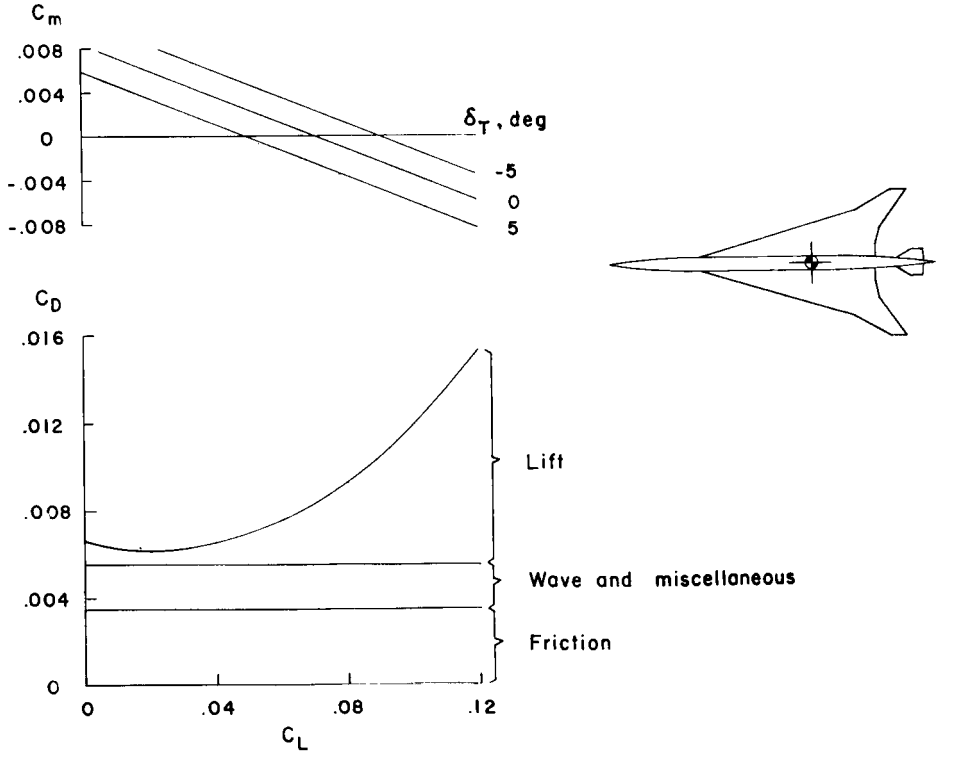


(b) Arrow-wing configuration.

Figure 6.- Cruise aerodynamic characteristics of SST designs at M = 2.7 and h = 18.3 km (60 000 ft).

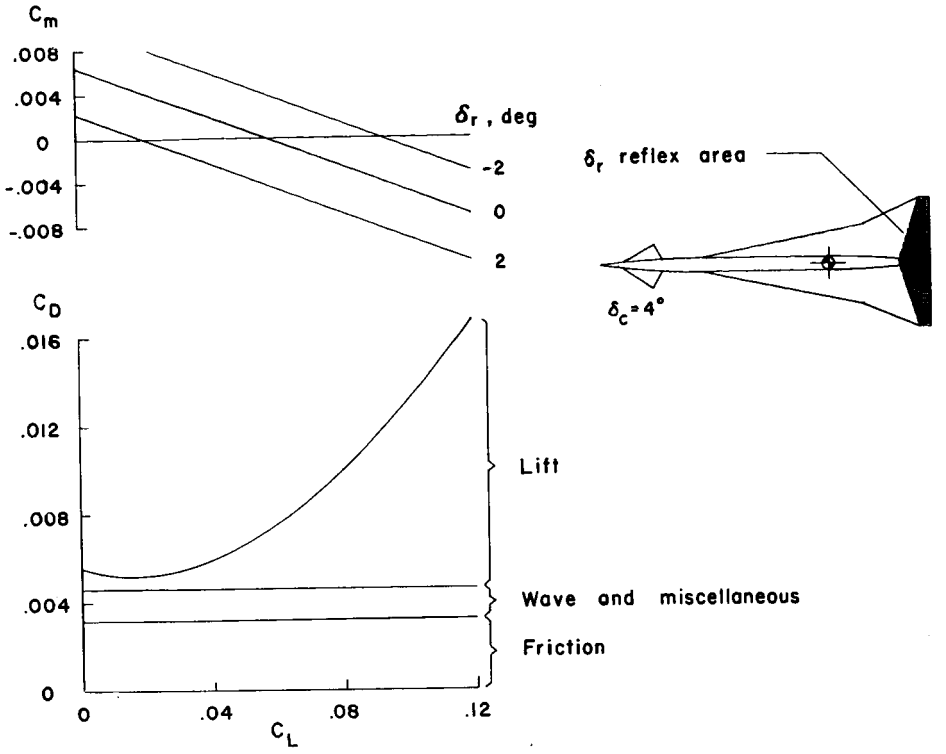


(c) Aft delta-wing configuration.

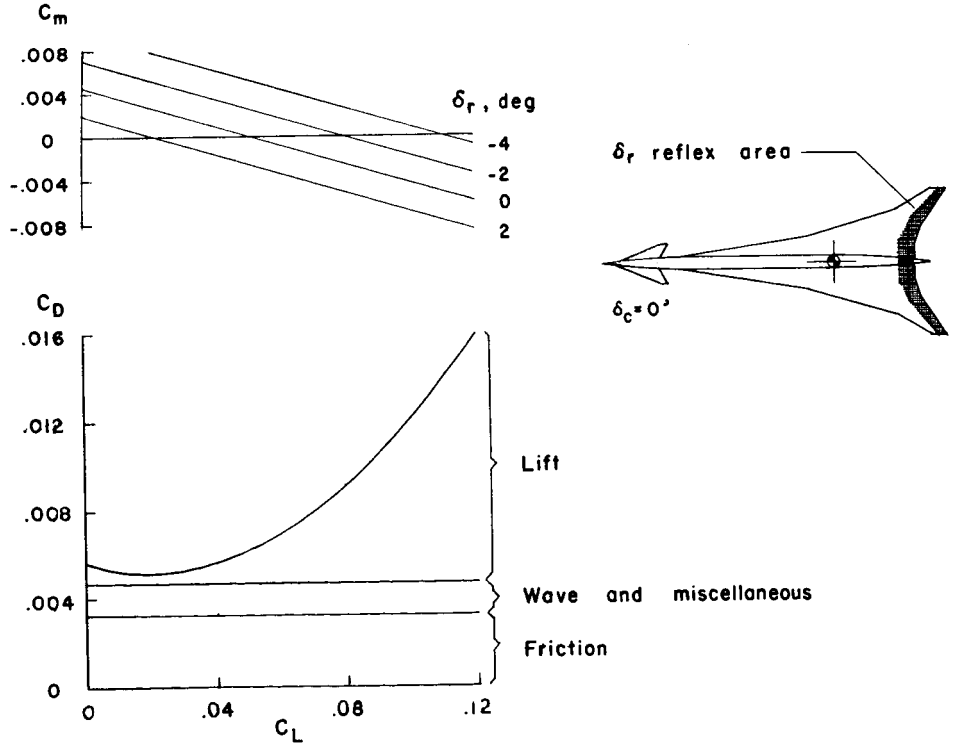


(d) Aft arrow-wing configuration.

Figure 6.- Concluded.

conventional delta-wing SST mission. Differences in supersonic-climb effective lift-drag ratios were based on the maximum lift-drag ratio at cruise Mach number, as given by the polars of figure 6. Differences in subsonic-climb effective lift-drag ratios were based on maximum lift-drag ratio at low speed as given by estimated polars which considered wetted area in determination of skin friction and equivalent delta-wing aspect ratio in determination of drag due to lift. Maximum lift-drag ratios for the four basic SST design concepts were considered to be as shown in the following table:

| SST design concept | $(L/D)_{max\ sub}$ | $(L/D)_{max\ sup}$ |
|---|---|---|
| Conventional delta | 13.6 | 7.3 |
| Conventional arrow | 13.3 | 8.8 |
| Aft delta | 12.3 | 8.2 |
| Aft arrow | 13.3 | 8.89 |

## PERFORMANCE AND WEIGHT ANALYSIS

Design-point airplane weights for the basic 2500-nautical-mile mission at $M = 2.7$ have been found by a process described in the following discussion and illustrated in figure 7.

The solid-line curves of figure 7 give the results of a performance analysis in terms of empty weight as a function of gross weight. With an assumed gross weight and the appropriate aerodynamic information as input data, the simplified performance analysis discussed previously and outlined in figure 4 is used to determine the corresponding empty weight. Curves are defined by a repetition of the process. Possible advances in propulsion technology are considered in curves obtained in a similar manner but with the constants in the performance equations multiplied by 0.9 for a 10-percent advance and by 0.8 for a 20-percent advance.

The dashed-line curves of figure 7 are obtained from the results of an airplane weight analysis discussed under "Study Methods." Examples of the airplane weight breakdown for an assumed gross weight of 272 000 kg (600 000 lbm) are given in table 4. Similar analysis for other gross weights permit definition of the dashed-line curve. Curves for weight technology advances are based on a 10-percent and a 20-percent reduction in airplane empty weight that might be brought about by improvements in materials or structural technology.

The design point is established by the intersection of the solid-line and dashed-line curves, the point at which both the performance analysis and the weight analysis are satisfied (fig. 7). Note that relatively small design gross-weight variations occur among

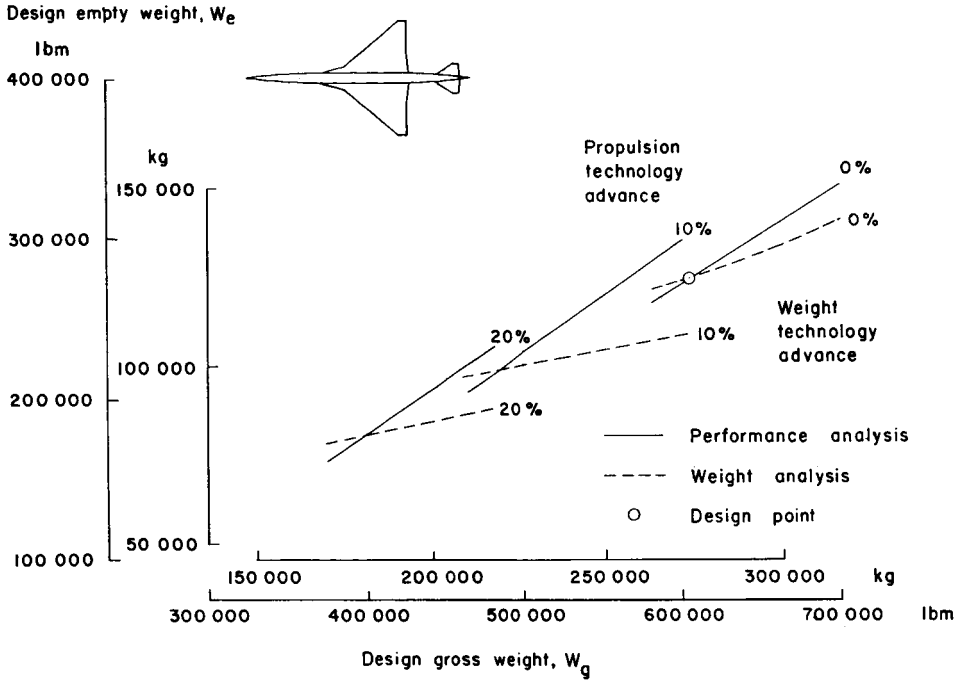


(a) Delta-wing configuration.

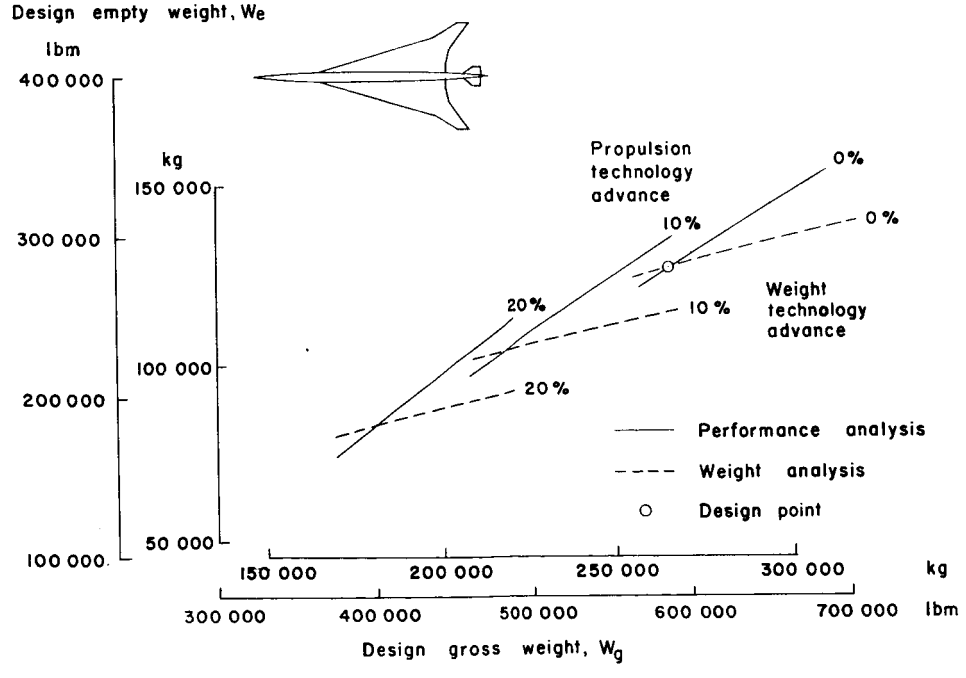


(b) Arrow-wing configuration.

Figure 7.- Design-point and advanced technology weight characteristics for basic SST designs.

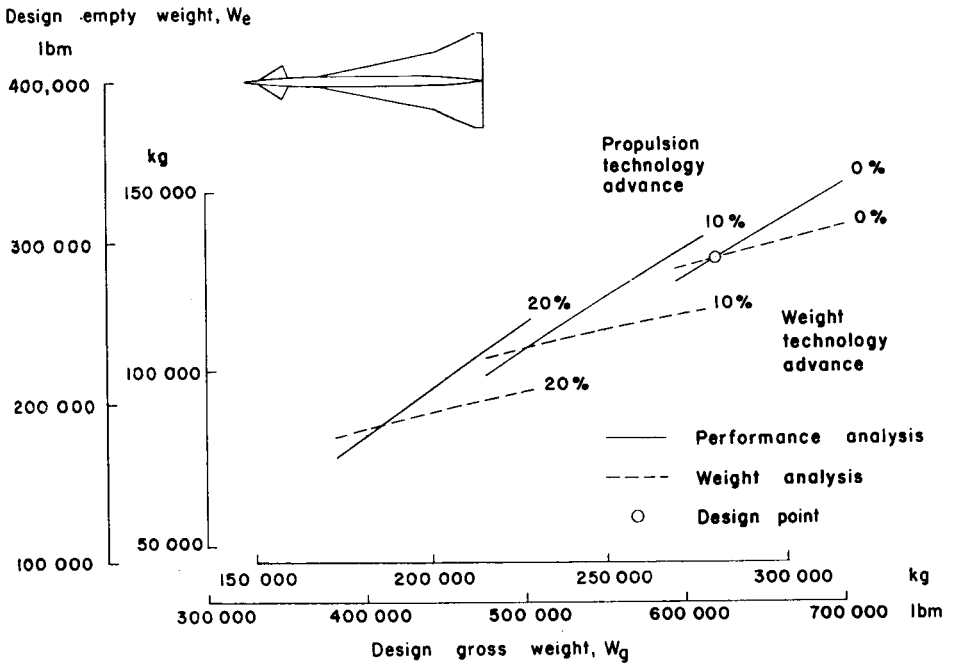


(c) Aft delta-wing configuration.

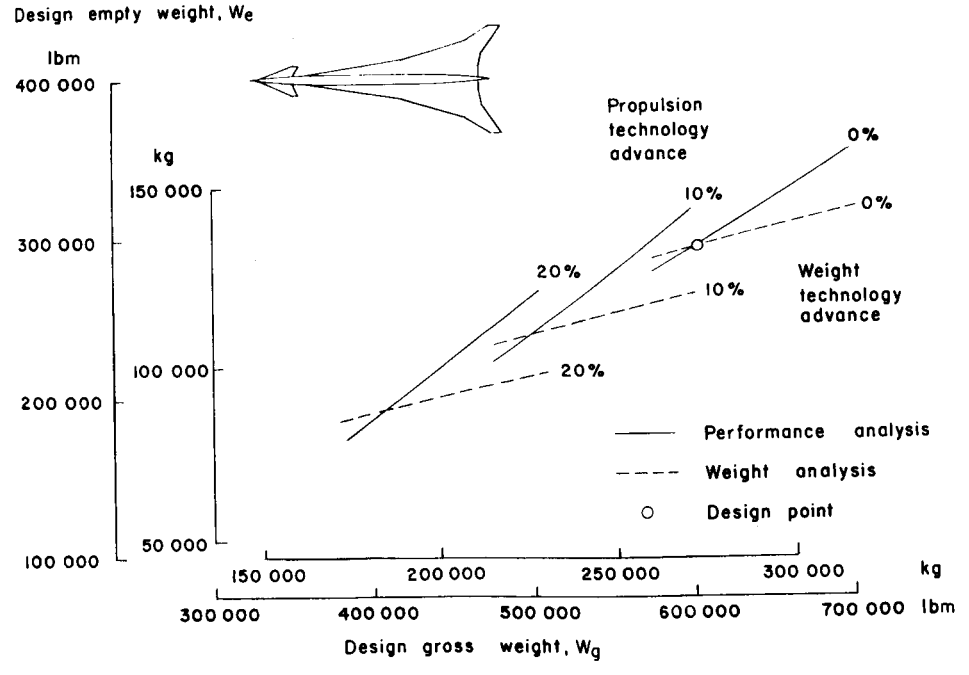


(d) Aft arrow-wing configuration.

Figure 7.- Concluded.

the four configurations (from 266 000 kg to 281 000 kg (586 000 lbm to 620 000 lbm)). Values for the conventional delta and conventional arrow designs are probably reasonably accurate, but values for the less conventional design concepts must be regarded with some skepticism because the superficial nature of the analysis may not anticipate problem areas.

## SONIC-BOOM ANALYSIS

### Design-Point Characteristics

Effective area developments used for the determination of pressure signatures for the basic SST design concepts are presented in figure 8. The volume contributions are obtained from a geometry subroutine of the wave drag program. The areas shown represent the frontal projection of the intersection of airplane components with cutting planes inclined at the Mach angle with respect to a horizontal plane. The equivalent area due to lift is determined from loading data from the wing programs and from weight and lift-coefficient data provided by the weights and performance analysis. This equivalent area is also determined by cutting planes inclined at the Mach angle and takes into account contributions from the cambered wing at angle of attack and from deflected control surfaces as well. The complete effective area formed from the sum of the volume and lift contributions is then used as an input to the sonic-boom program described in the section entitled "Theoretical Considerations."

Predicted nominal ground track signatures for the design point of $M = 2.7$ and an altitude of 18.3 km (60 000 ft) are shown in figure 9. Corresponding effective area developments are shown in inset sketches. Results for the basic configurations as described in tables 1 and 2 are shown by the solid-line curve. Results attainable by rather modest modifications of the basic design concepts are indicated by the dashed-line curves. Suitable alterations might be accomplished by a revision of the fuselage area development, by selection of a wing dihedral or shear profile, by redefinition of the wing camber surface, or by relocation and resizing of the control surfaces. Minor redesign of any of the configurations to satisfy effective area development requirements is expected to introduce little or no penalty in aerodynamic characteristics or in airplane performance. For the conventional design approaches there would probably be some loss in seating capacity, but for the sonic-boom designs care was taken in the initial configurating to minimize the need for subsequent revisions.

Note that for the conventional delta-wing design concept (fig. 9(a)), even with appreciable redesign, the far-field N-wave characteristic of the signature remains and a shock strength of about 110 $N/m^2$ (2.3 $lbf/ft^2$) is predicted. For the conventional arrow-wing design (fig. 9(b)), shock strength is somewhat less, about 84 $N/m^2$ (1.75 $lbf/ft^2$). In

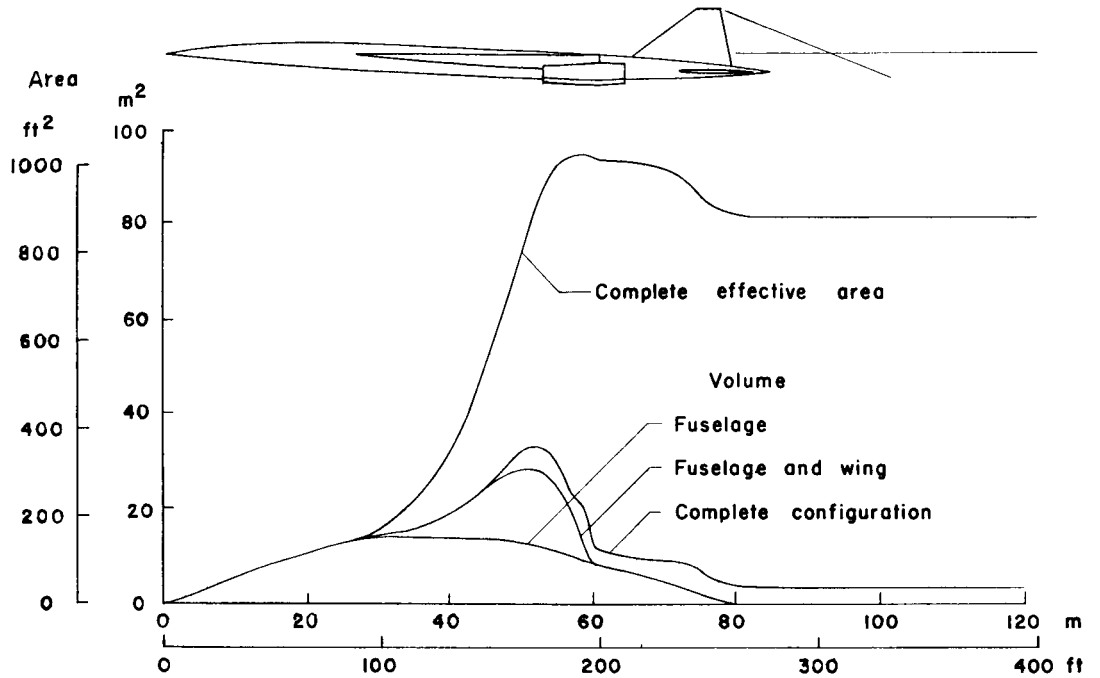


(a) Delta-wing configuration; $W_c$ = 234 000 kg (518 000 lbm).

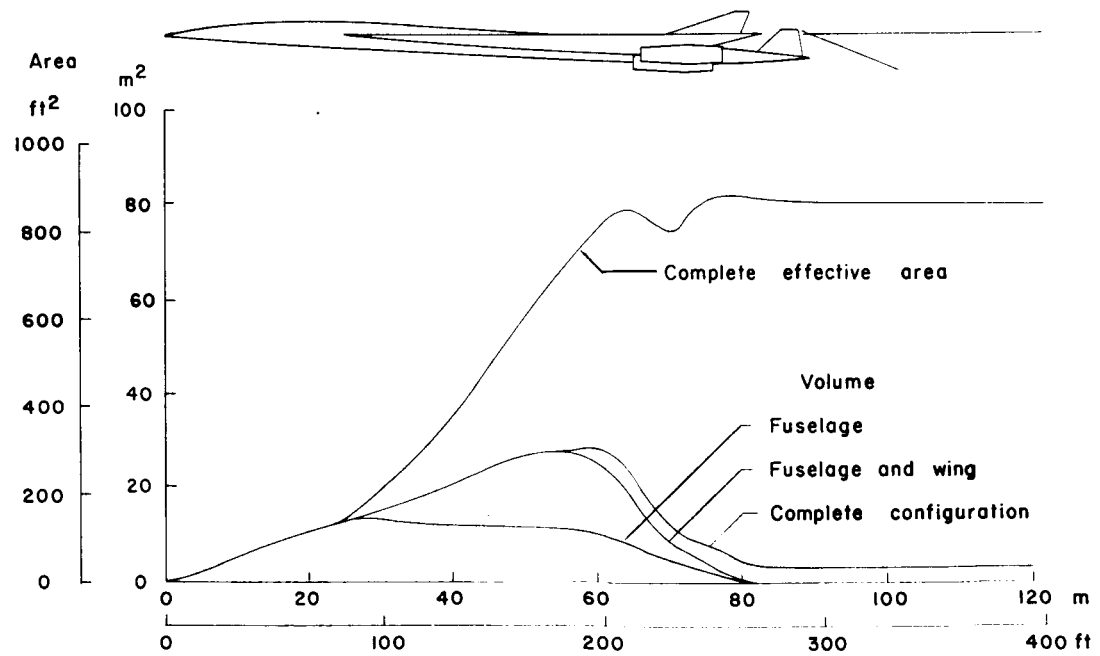


(b) Arrow-wing configuration; $W_c$ = 230 000 kg (509 000 lbm).

Figure 8.- Design-point effective area development for basic SST designs at M = 2.7 and h = 18.3 km (60 000 ft).

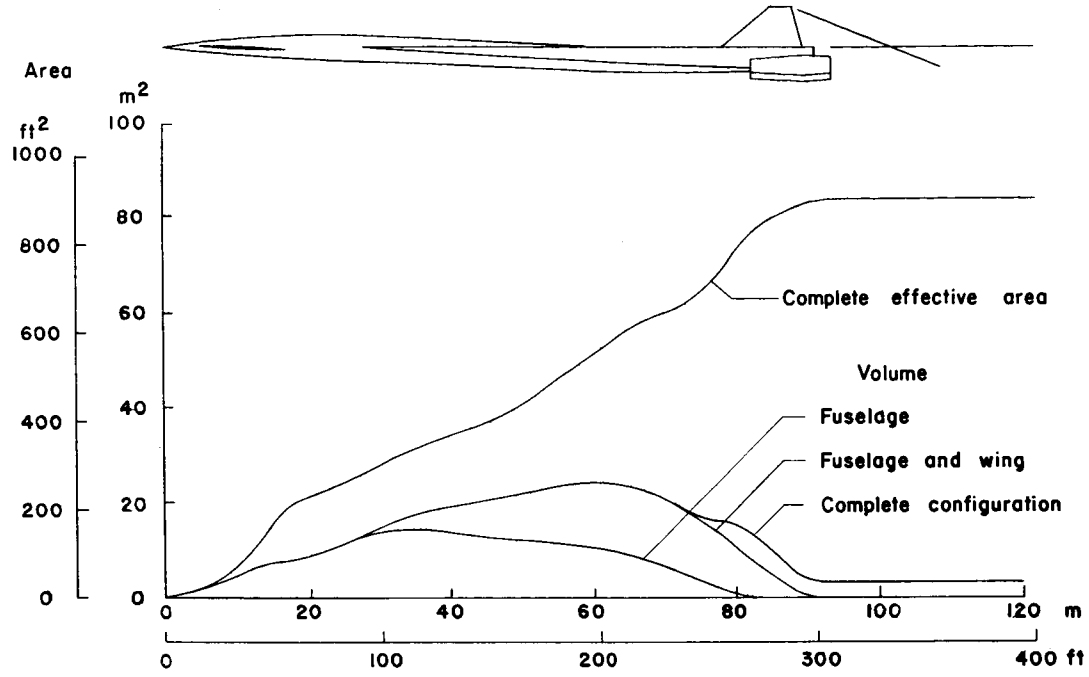


(c) Aft delta-wing configuration; $W_c$ = 242 000 kg (534 000 lbm).

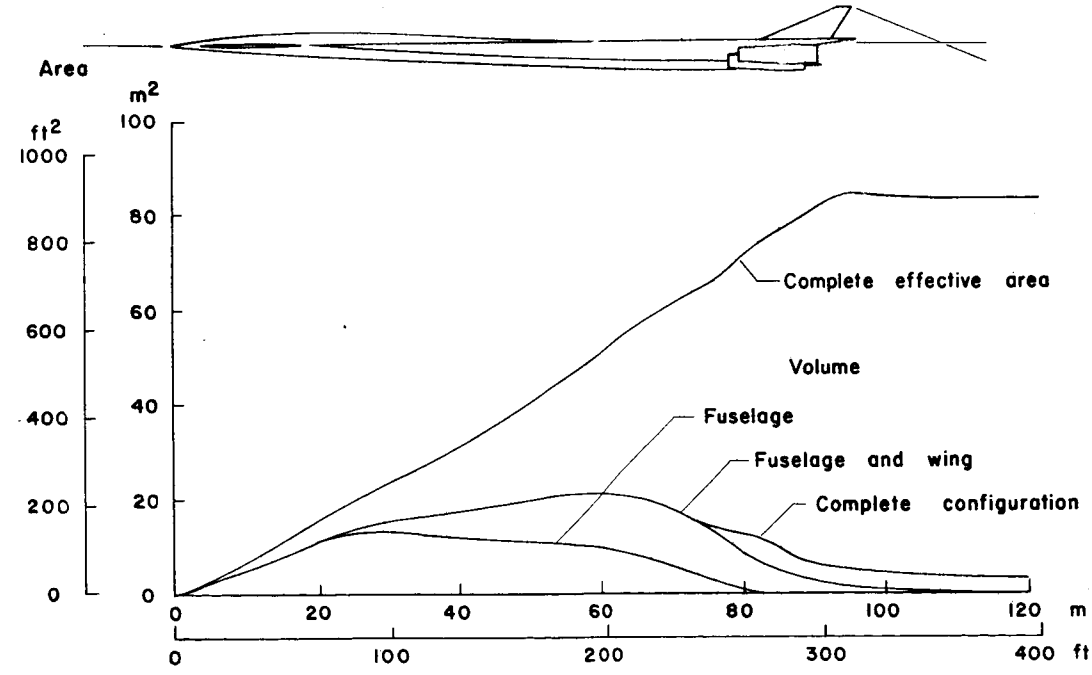


(d) Aft arrow-wing configuration; $W_c$ = 239 000 kg (527 000 lbm).

Figure 8.- Concluded.

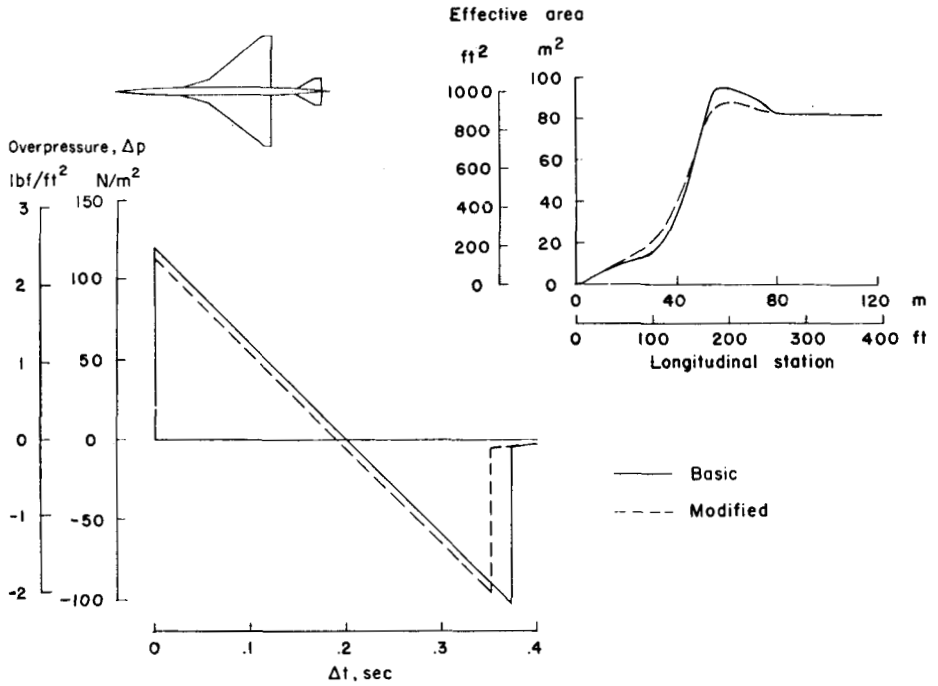


(a) Delta-wing configuration; $W_c$ = 234 000 kg (518 000 lbm).

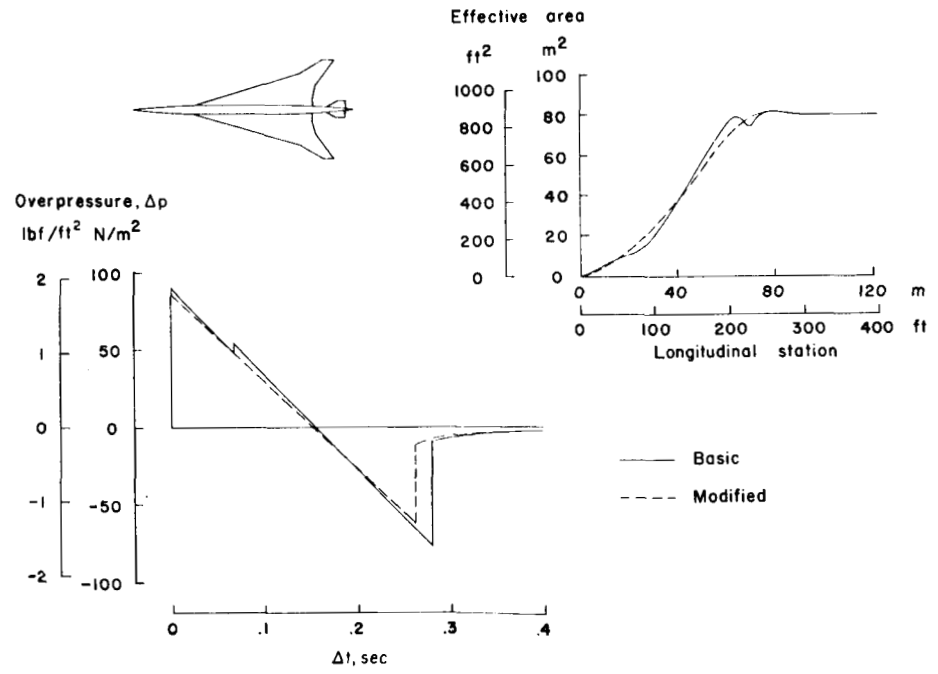


(b) Arrow-wing configuration; $W_c$ = 230 000 kg (509 000 lbm).

Figure 9.- Design-point sonic-boom signatures for basic and modified design at M = 2.7 and h = 18.3 km (60 000 ft).

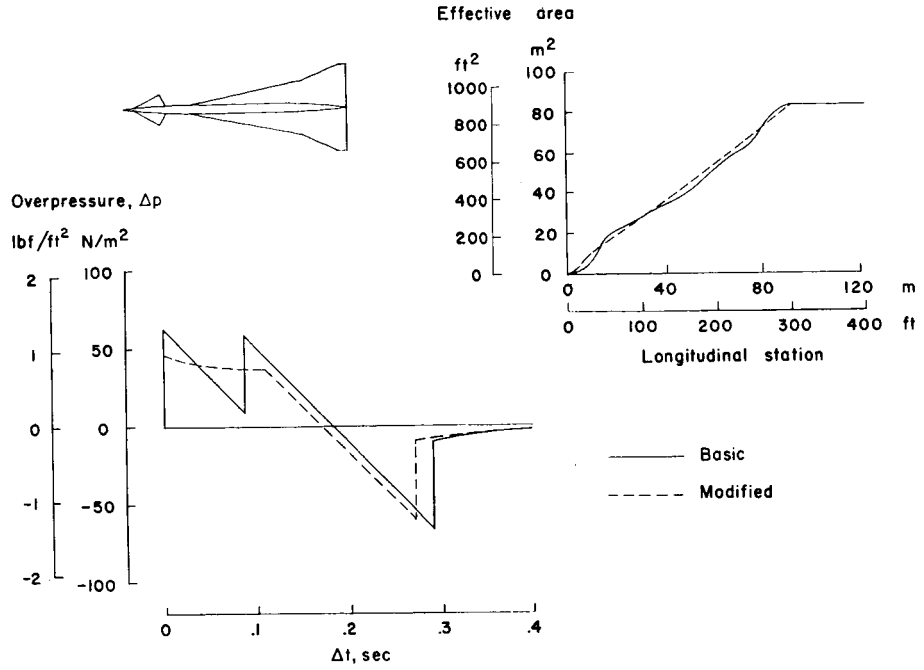


(c) Aft delta-wing configuration; $W_c$ = 242 000 kg (534 000 lbm).

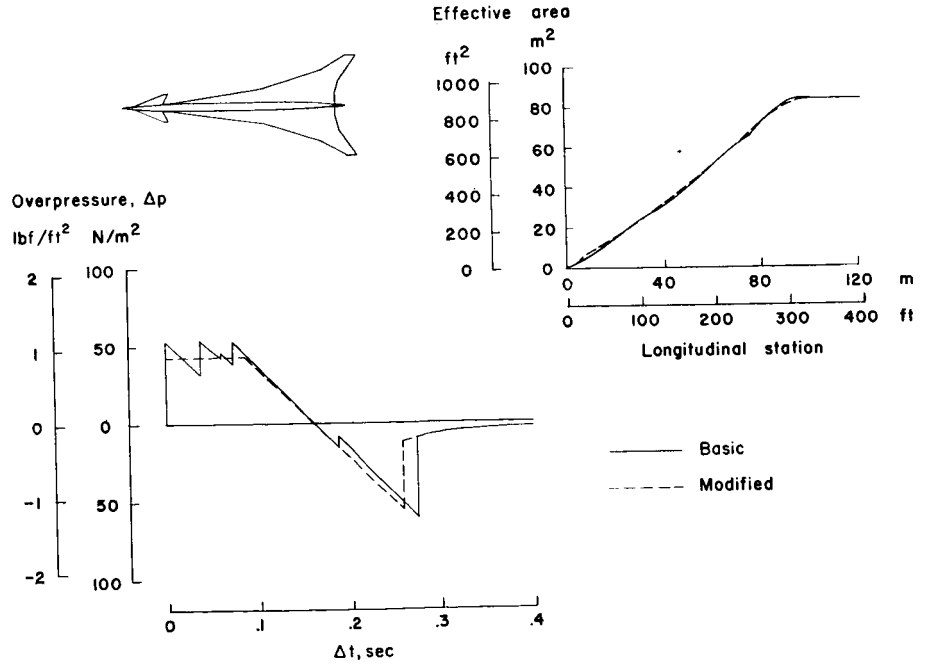


(d) Aft arrow-wing configuration; $W_c$ = 239 000 kg (527 000 lbm).

Figure 9.- Concluded.

contrast, the sonic-boom-controlled designs (figs. 9(c) and 9(d)) have predicted bow shock strengths of less than 48 $N/m^2$ (1.0 $lbf/ft^2$). The tail shock strength for the aft delta-wing design, however, is slightly larger than the bow shock and thus becomes the controlling factor.

There can be no assurance at this time that shock-strength values less than 48 $N/m^2$ (1.0 $lbf/ft^2$), if attainable, would permit unrestricted overland operations of supersonic transports. Study results however do offer sufficient encouragement to warrant a renewed effort to define more accurately the acceptability of near-field signatures in the 24- to 48-$N/m^2$ (0.5- to 1.0-$lbf/ft^2$) shock-strength range.

Commitment to an airplane development program based on employment of these sonic-boom minimization concepts would be dependent on confirmation of theoretical predictions in carefully planned and conducted wind-tunnel test programs. There is, however, believed to be sufficient validity to the basic theory to insure that sonic-boom characteristics reasonably close to those predicted would be attainable with sufficient attention to detail in an experimental fine-tuning effort. A larger question concerns the practicality of incorporating effective sonic-boom design features in airplanes that meet the technical and economic requirements for airline operations.

### Influence of Altitude

In an effort to define an optimum cruise altitude from the sonic-boom standpoint, the aerodynamic, weight, performance, and sonic-boom analyses were repeated for two additional altitudes. Results are presented in figure 10. Shock strength (bow or tail, whichever is greater) is given as a function of cruise altitude. For each condition studied, freedom in modifying the basic design for sonic-boom benefits was exercised to about the same degree as for the design-point cases previously discussed. Inset sketches show the modified effective area developments and the corresponding pressure signatures. For both conventional design approaches, which produce far-field N-wave signatures, shock strength continues to decrease with altitude over the range shown, with little or no penalty in fuel consumption. This result, however, must be somewhat suspect because no detailed analysis was made for the climb fuel.

For both sonic-boom designs, which are configured to produce near-field signatures, an optimum altitude is found at 16 to 18 km (53 000 to 59 000 ft). Sonic-boom benefits associated with cruising flight below the maximum lift-drag-ratio altitude (which, for example, occurs at about 20 km (64 000 ft) for the aft arrow-wing design) are however found to be slight. Decreases in aerodynamic efficiency and increases in fuel requirements rapidly overcome any benefit of increased near-field characteristics.

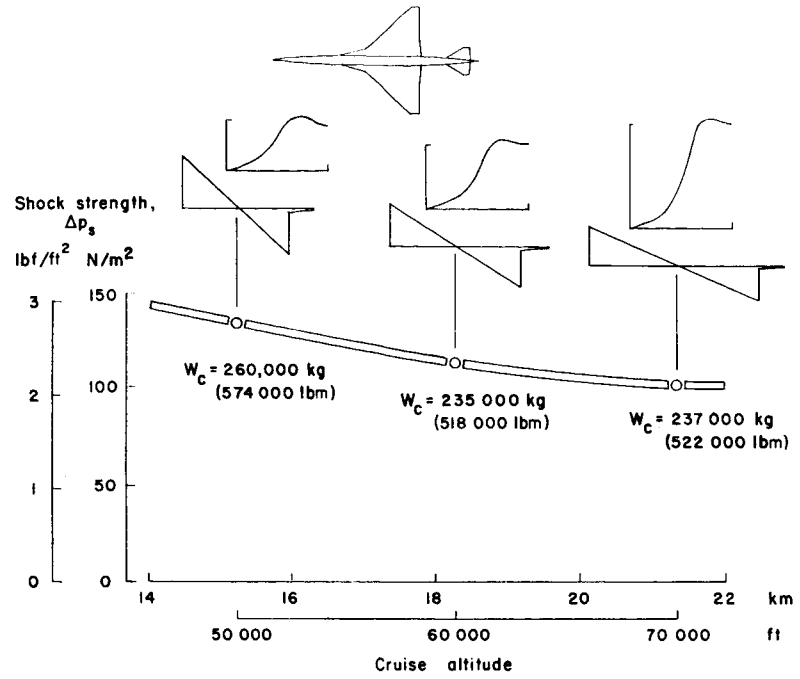


(a) Delta-wing configuration.

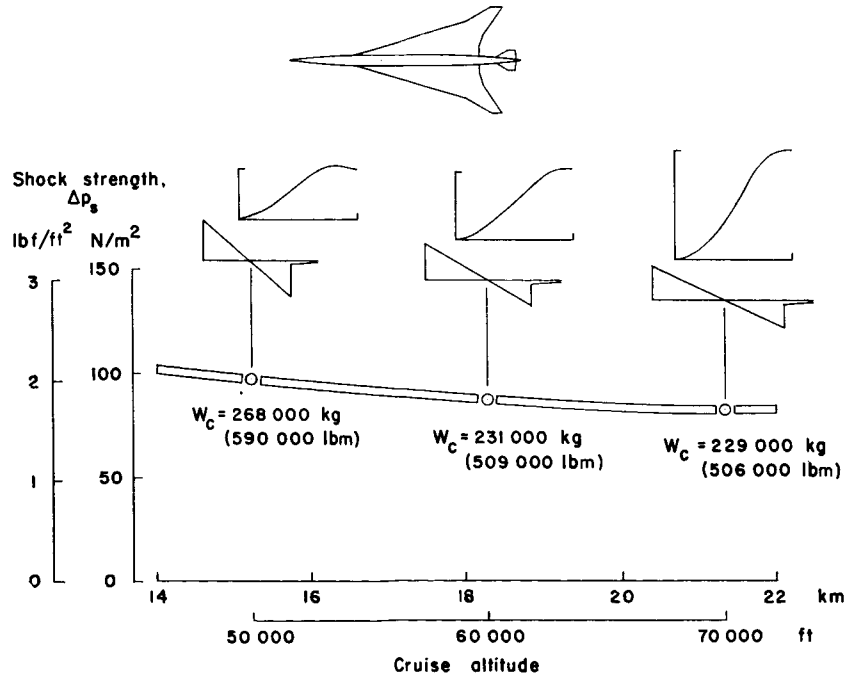


(b) Arrow-wing configuration.

Figure 10.- Influence of cruise altitude on shock strength for sonic-boom modified SST designs at M = 2.7.

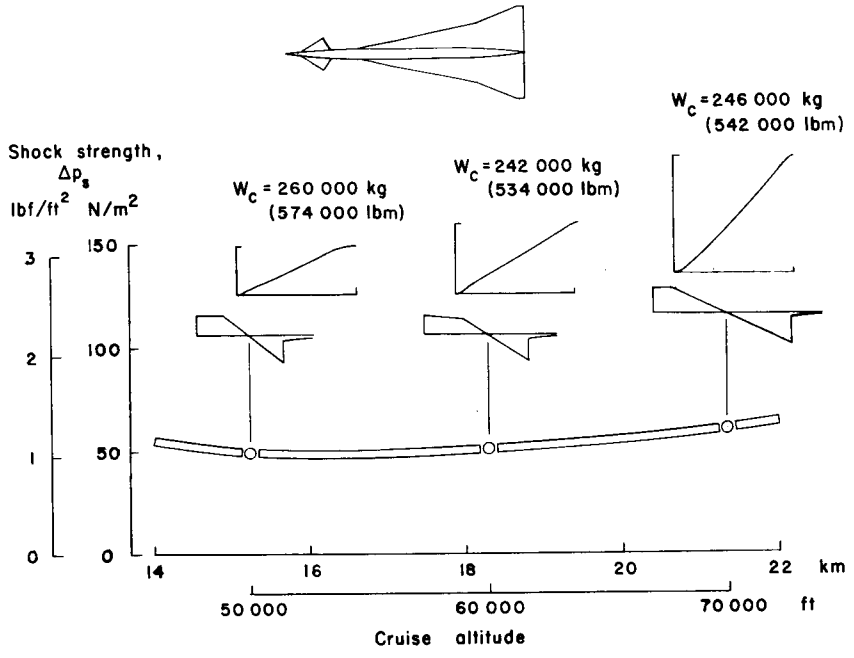


(c) Aft delta-wing configuration.

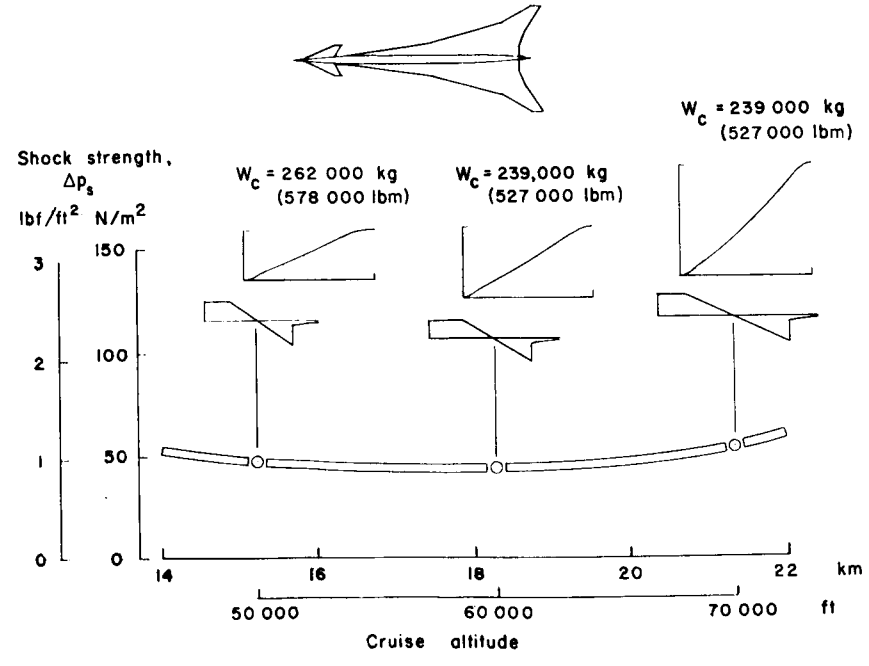


(d) Aft arrow-wing configuration.

Figure 10.- Concluded.

## Influence of Technology Advances

An important consideration that often arises in discussions of sonic-boom minimization is the advantage that can be taken of across-the-board technology advances. As indicated in the section entitled "Performance and Weight Analysis," design-point airplane weights were also evaluated for combined empty weight and specific fuel-consumption reductions of 10 and 20 percent. The influence of these potential weight reductions on shock-strength values is illustrated in figure 11. Again, inset sketches are used to show modified effective area developments and signatures corresponding to each condition studied. For convenience, curves for the four design concepts (without the sketches) are combined in figure 12. It can be seen that, although technology advances offer appreciable gains for conventional design approaches, these gains are not comparable with those potentially attainable through the employment of sonic-boom-controlled design approaches.

## Sensitivity Studies

Studies have been made of certain design parameters believed to exert a strong influence on sonic-boom characteristics for boom-optimized designs. These parameters include canard angle, dihedral angle, center of gravity, and aerodynamic efficiency.

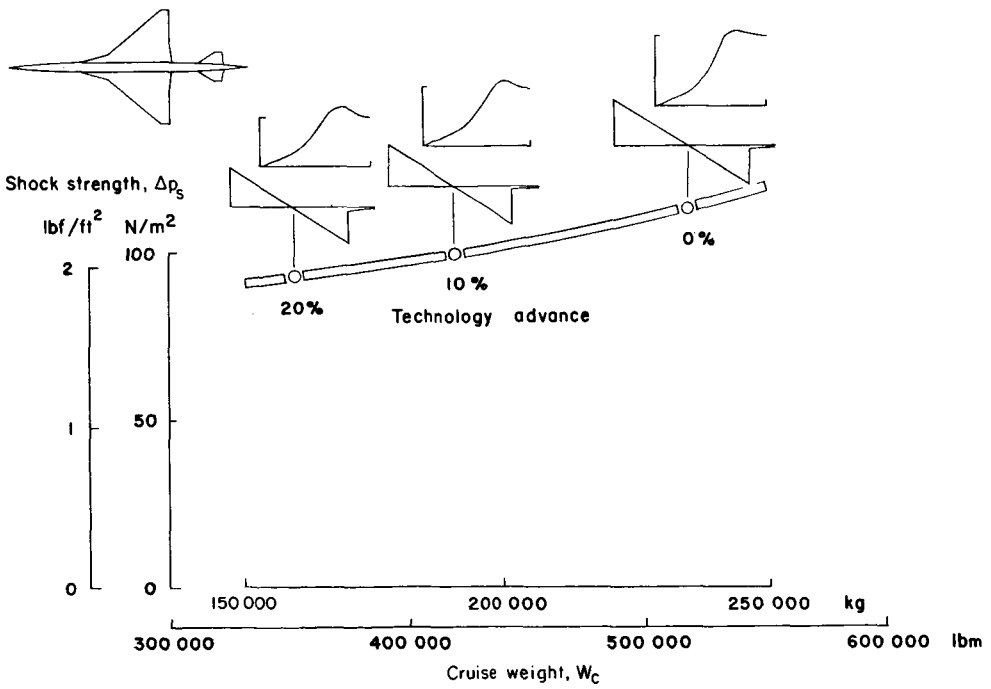


(a) Delta-wing configuration.

Figure 11.- Influence of cruise weight on shock strength for sonic-boom modified SST designs at M = 2.7 and h = 18.3 km (60 000 ft).

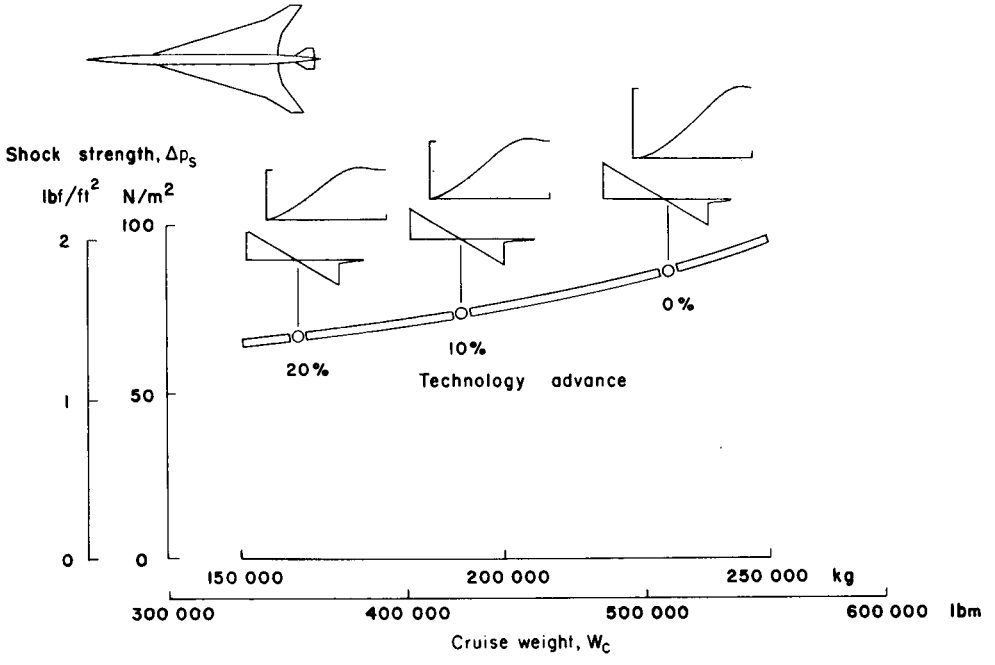


(b) Arrow-wing configuration.

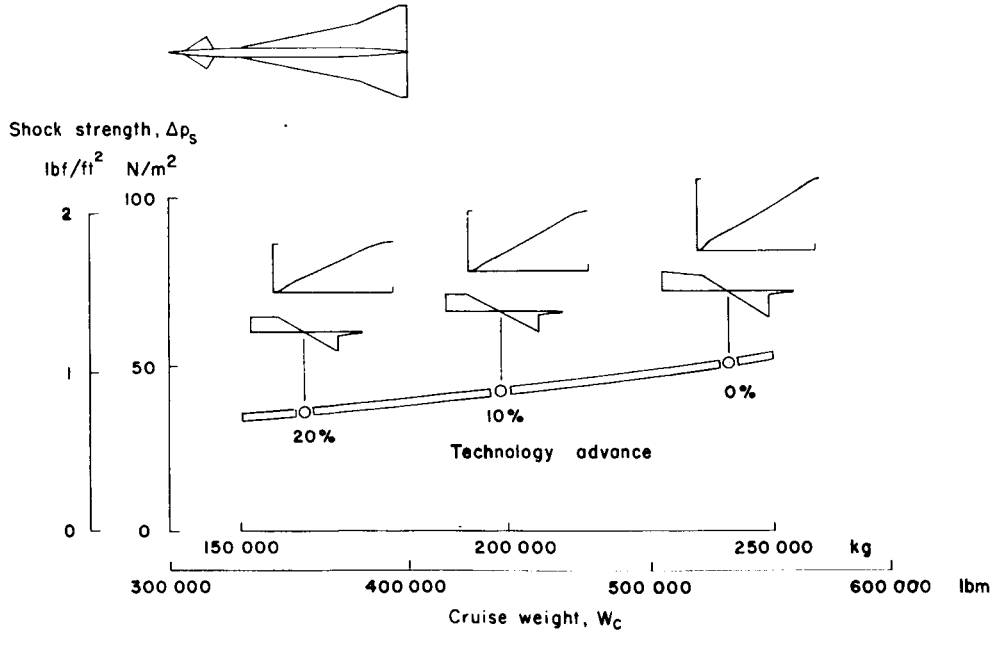


(c) Aft delta-wing configuration.

Figure 11.- Continued.

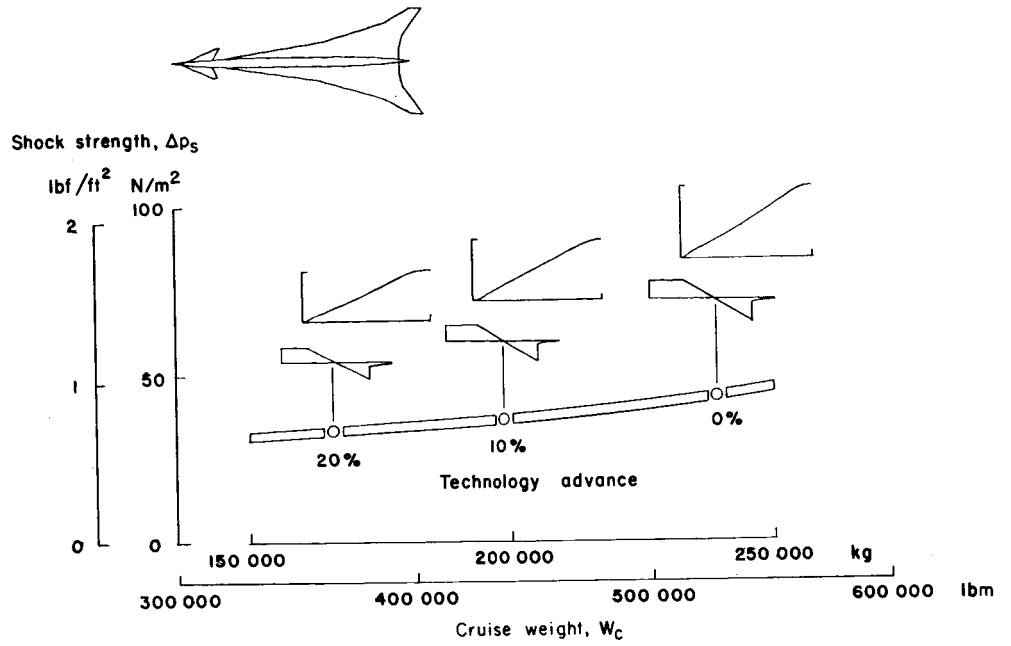


(d) Aft arrow-wing configuration.

Figure 11.- Concluded.

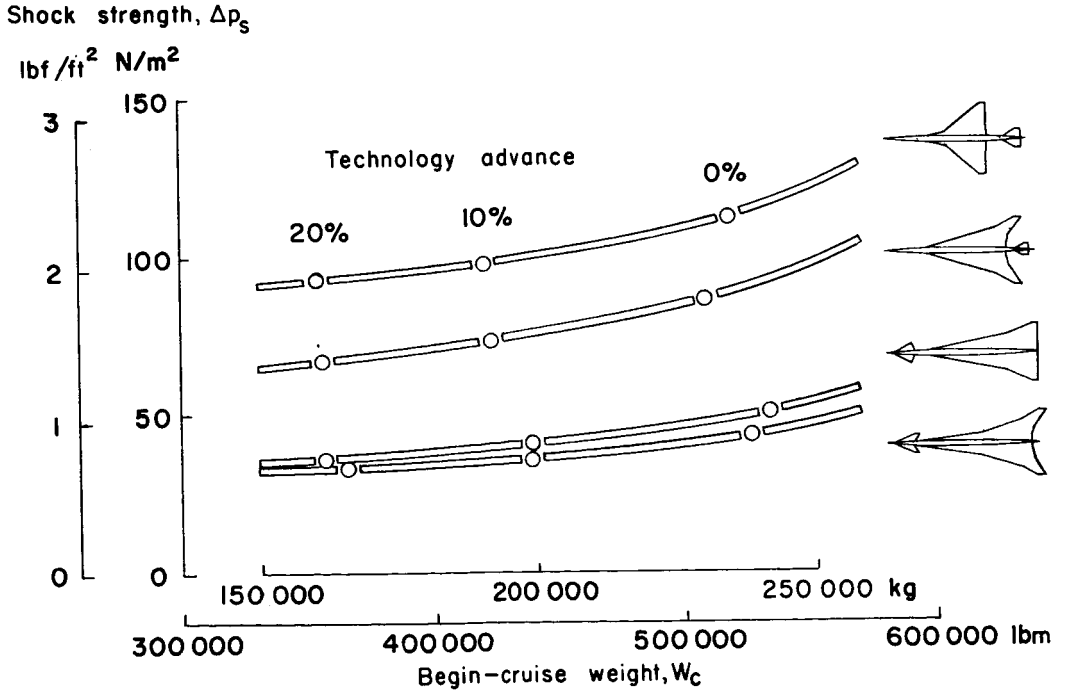


Figure 12.- Comparison of results from different approaches to sonic-boom minimization at M = 2.7 and h = 18.3 km (60 000 ft).

The influence of canard setting on shock strength is illustrated in figure 13. For the aft delta-wing design concept, canard setting is seen to optimize at an incidence of about $3^{\circ}$ or $4^{\circ}$. At this condition the rather abrupt beginning of the effective area development yields a spike in the F-function which is not felt in the shock but which serves to reduce the overpressure in the plateau region of the signature. The canard appears to be an important design feature of this particular configuration. As shown in figure 13(b) the arrangement of the aft arrow-wing design concept considered in the study does not appear to have the same requirement for lift carried by the canard. Sonic-boom characteristics at an optimum setting near $1^{\circ}$ or $2^{\circ}$ are little different from those with the canard at $0^{\circ}$. Because canard volume contributions are almost negligible, the results at $\delta_c = 0^{\circ}$ are indicative of sonic-boom characteristics attainable for a similar design in which the canard is omitted. Sonic-boom benefits at larger canard angles might be achieved except for the bend in the aft portion of the effective area development resulting from the increased loading of the wing reflex area required to counteract the canard lift and provide trim. Other component arrangements might permit better advantage to be made of the sonic-boom reduction potential of canard lift.

As shown in figure 14, dihedral angle is an extremely important design consideration. Dihedral angle is defined as shown in the sketch of the rear view of the configuration at its design attitude. A dihedral angle of $0^{\circ}$ would result in a shock strength of about

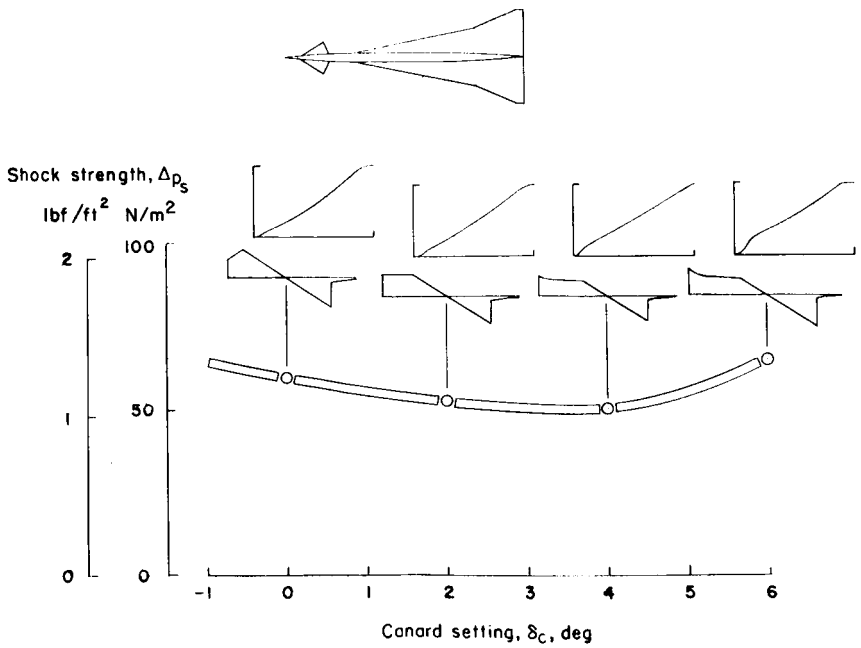


(a) Modified aft delta-wing configuration.

Figure 13.- Influence of canard setting on shock strength for sonic-boom modified SST designs at M = 2.7 and h = 18.3 km (60 000 ft).

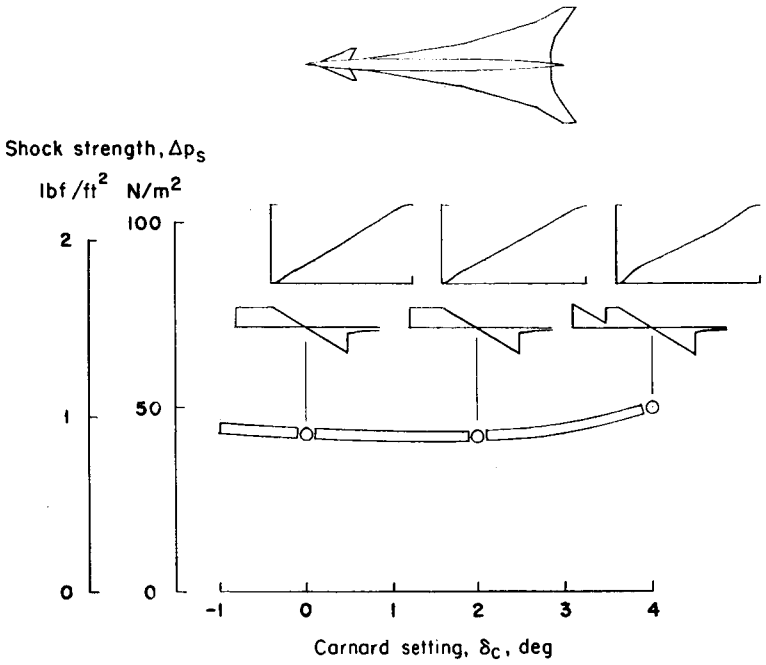


(b) Modified aft arrow-wing configuration.

Figure 13.- Concluded.

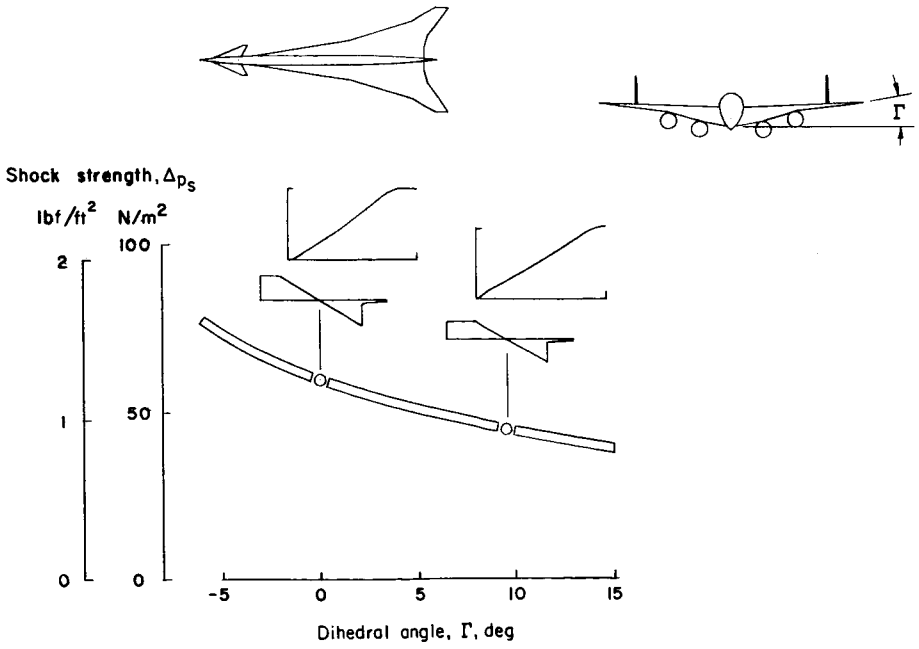


Figure 14.- Influence of dihedral angle on shock strength for sonic-boom modified aft arrow-wing SST design at M = 2.7 and h = 18.3 km (60 000 ft).

61 N/m$^2$ (1.25 lbf/ft$^2$). A dihedral angle of about 9.5$^o$ permits the trailing edge of the wing tip to lie in the same horizontal plane as the wing apex and prevents Mach plane foreshortening. The 9.5$^o$ dihedral is equivalent to about a 12-meter (40-foot) increase in the wing overall length and results in a 28-percent reduction in shock strength to about 43 N/m$^2$ (0.9 lbf/ft$^2$). Increased dihedral could lead to greater gains. There is thus a strong incentive for solution of the problem of roll-yaw coupling for wings with positive dihedral. The quoted values of shock strength significantly less than 48 N/m$^2$ (1.0 lbf/ft$^2$) given in this paper are valid only if it can be presumed that such a solution will be found.

Because of uncertainties in the estimated center-of-gravity positions of the less conventional design concepts, a sensitivity study was performed for the aft arrow-wing design. Results are shown in figure 15. For each center-of-gravity position studied, freedom in modifying the basic design for sonic-boom benefits was exercised to about the same degree as for the design-point cases previously discussed. Inset sketches again show the modified area developments and the signatures. The assumed design-point center-of-gravity location corresponded to the 46-percent station of the mean aerodynamic chord. It is seen that for a fairly broad region, between 40 and 50 percent of the mean aerodynamic chord, sonic-boom results would not be far different. Increased shock strength for forward center-of-gravity locations is caused by the negative loading required on the wing reflex area to provide trim and by poorer aerodynamic efficiency

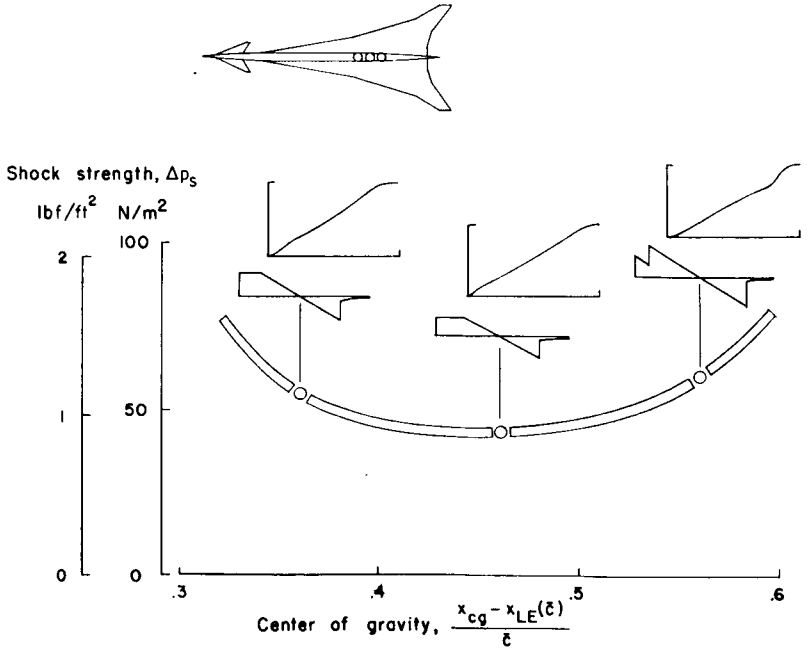


Figure 15.- Influence of center-of-gravity location on shock strength for sonic-boom modified aft arrow-wing SST design at M = 2.7 and h = 18.3 km (60 000 ft).

resulting in weight penalties. A large positive loading of the wing reflex area in combination with an unloaded canard was required to provide trim for the rear center-of-gravity location. The modification of the effective area development was as large as consistency with other cases would allow and still was not sufficient to prevent formation of a double bow shock and a strong tail shock.

The influence of aerodynamic efficiency may be assessed in a rather simple way. Various values of lift-drag ratios may be used in the simplified performance analysis to establish airplane weights, and overpressures corresponding to these weights may be read from charts such as those shown in figure 11. Results of such a study given in figure 16 are somewhat surprising. Neither appreciable gains associated with substantial improvements in lift-drag ratio nor appreciable penalties associated with reasonable degradations are found. Propulsion and materials technology are found to be of greater importance in attacking the sonic-boom problem.

## Airplane Growth for Increased Range

The primary emphasis of this study is placed on supersonic transports designed for a payload of 21 800 kg (48 000 lbm) and a U.S. transcontinental range of 2500 nautical miles in the belief that there would be a substantial market for such a vehicle and that such restrictions would permit the achievement of acceptable sonic-boom characteristics.

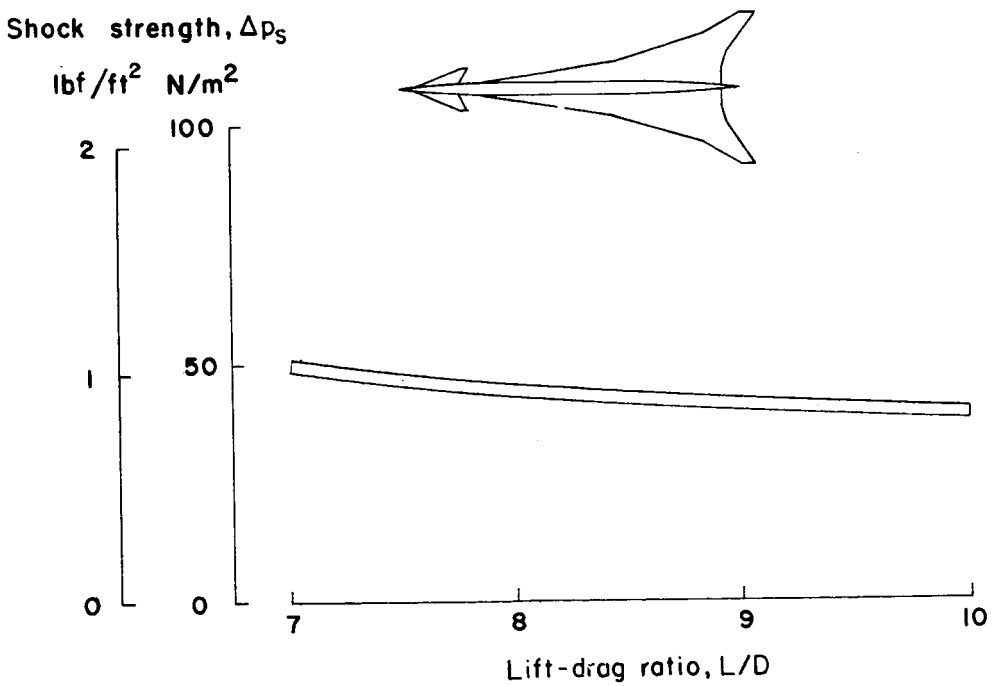


(a) Supersonic efficiency.

Figure 16.- Influence of aerodynamic efficiency on shock strength for sonic-boom modified aft arrow-wing SST design at M = 2.7 and h = 18.3 km (60 000 ft).

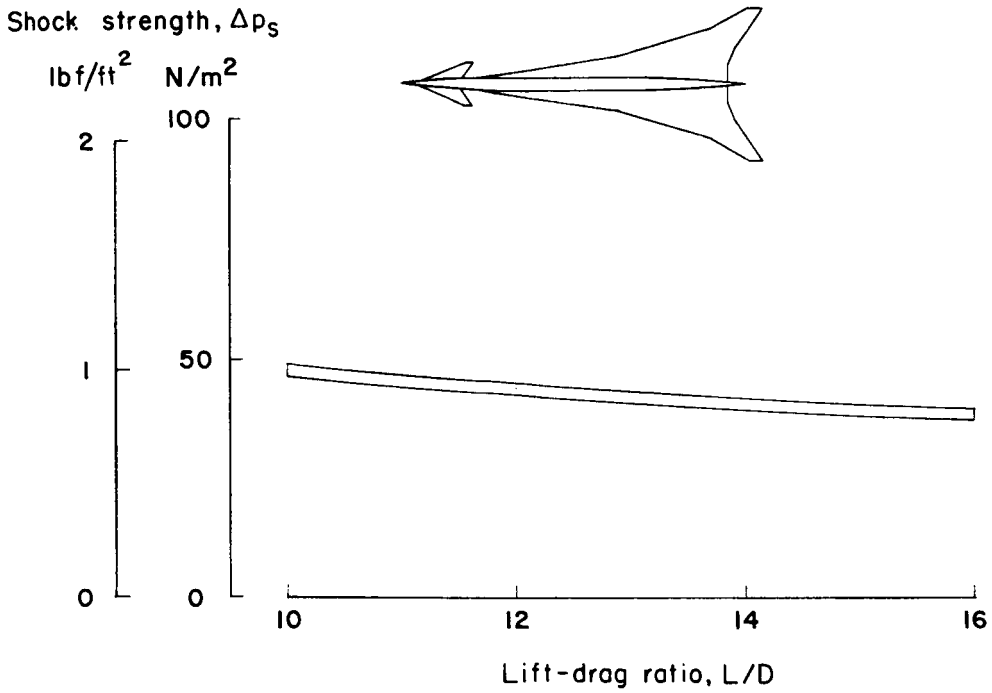


(b) Subsonic efficiency.

Figure 16.- Concluded.

There are however compelling economic reasons for greater range capabilities so that one airplane will serve for both intercontinental and transcontinental missions. Because of this concern, calculations were performed for the aft arrow-wing design to determine the gross weight and the sonic-boom characteristics for a 3500-nautical-mile-range airplane. Results are presented in figure 17. With the full fuel complement for a 3500-nautical-mile flight the airplane would have a gross weight of about 335 000 kg (740 000 lbm) and at the beginning of cruise would produce a shock strength of about 62 N/m$^2$ (1.3 lbf/ft$^2$) if the sonic-boom design was based on that condition. It might be desirable, however, to base the sonic-boom shaping on the begin-cruise conditions for an off-loaded airplane with fuel for a 2500-nautical-mile mission. In that case, shock-strength values would be about 53 N/m$^2$ (1.1 lbf/ft$^2$). Thus, a heavier airplane capable of both intercontinental and transcontinental missions could be used on transcontinental missions with about a 20-percent increase in sonic-boom overpressures. This result however is contingent on a center of gravity maintained at the same location as for the shorter range airplane; this may prove to be difficult if aft portions of the wing volume are required for fuel storage.

## Comparison of Design Concepts

A comparison of the estimated sonic-boom minimization potential associated with each design approach is given in figure 18. In this comparison, each design is allowed

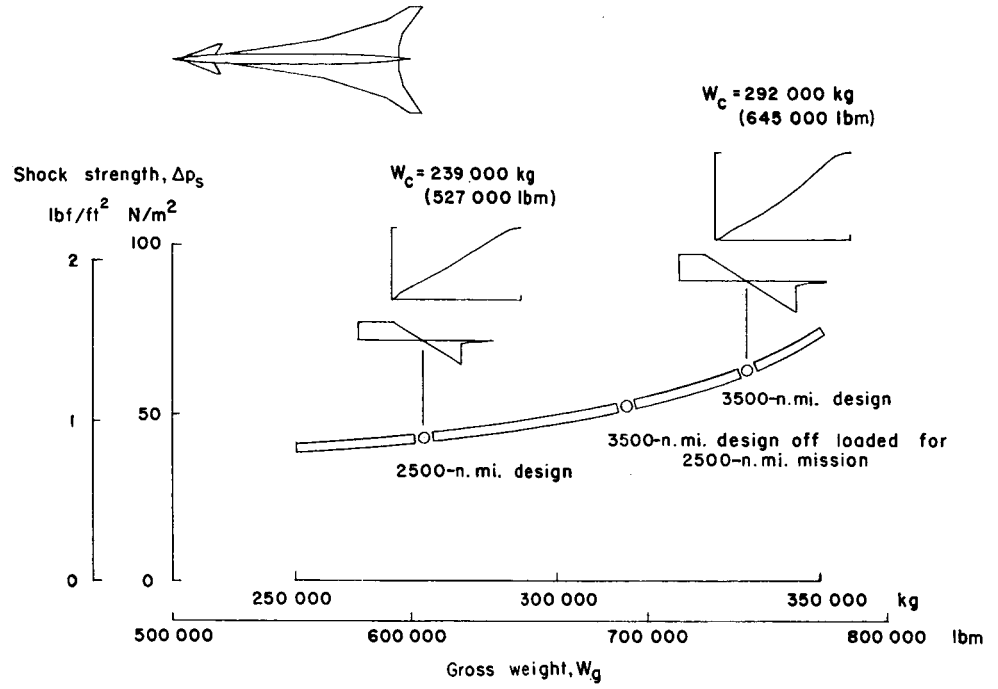


Figure 17.- Influence of growth in airplane gross weight on shock strength for sonic-boom modified aft arrow-wing SST design at M = 2.7 and h = 18.3 km (60 000 ft).

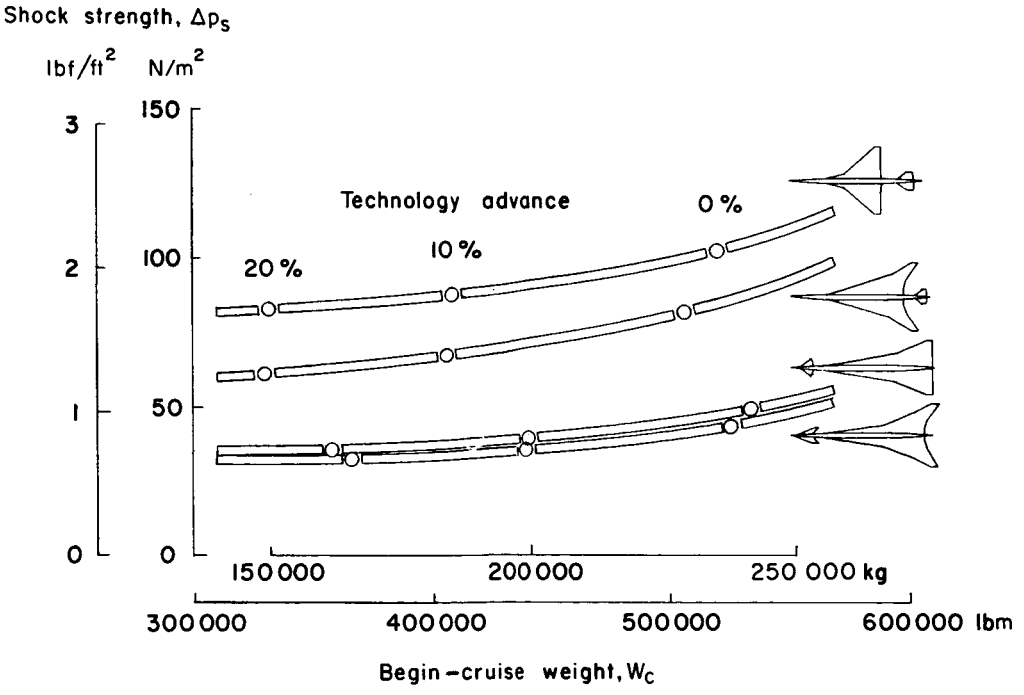


Figure 18.- Estimated potential for different approaches to sonic-boom minimization. M = 2.7.

to fly at an altitude that minimizes shock strength even though weight and economics may be sacrificed. Allowance is also made for minor configuration changes, such as canard relocation or wing camber modifications, to permit simultaneous improvement in trim characteristics and sonic-boom shaping. Although technology advances offer appreciable gains for conventional design approaches, these gains are not comparable with those potentially attainable through departures from conventional design practices based on sonic-boom considerations. Shock-strength levels of about 36 $N/m^2$ (0.75 $lbf/ft^2$) are indicated if full advantage can be taken of technology advances in structural design concepts, materials, and propulsion.

To summarize the comparison of the design concepts, shock strength may be related in a general way to the effective length of the airplane lifting surface as shown in figure 19. The importance of increased effective lifting length gained by long root chords, by trailing-edge sweep, by wing dihedral, and by use of a lifting canard is obvious. It is significant that the conventional arrow-wing design, which already has been given serious consideration as a candidate SST design, lies at the knee of the curve, where near-field effects begin to appear. Further increases in effective length could bring about sizable sonic-boom benefits. If the results of this study are to be believed, appreciable weight increases do not accompany increased effective length for the advanced designs shown.

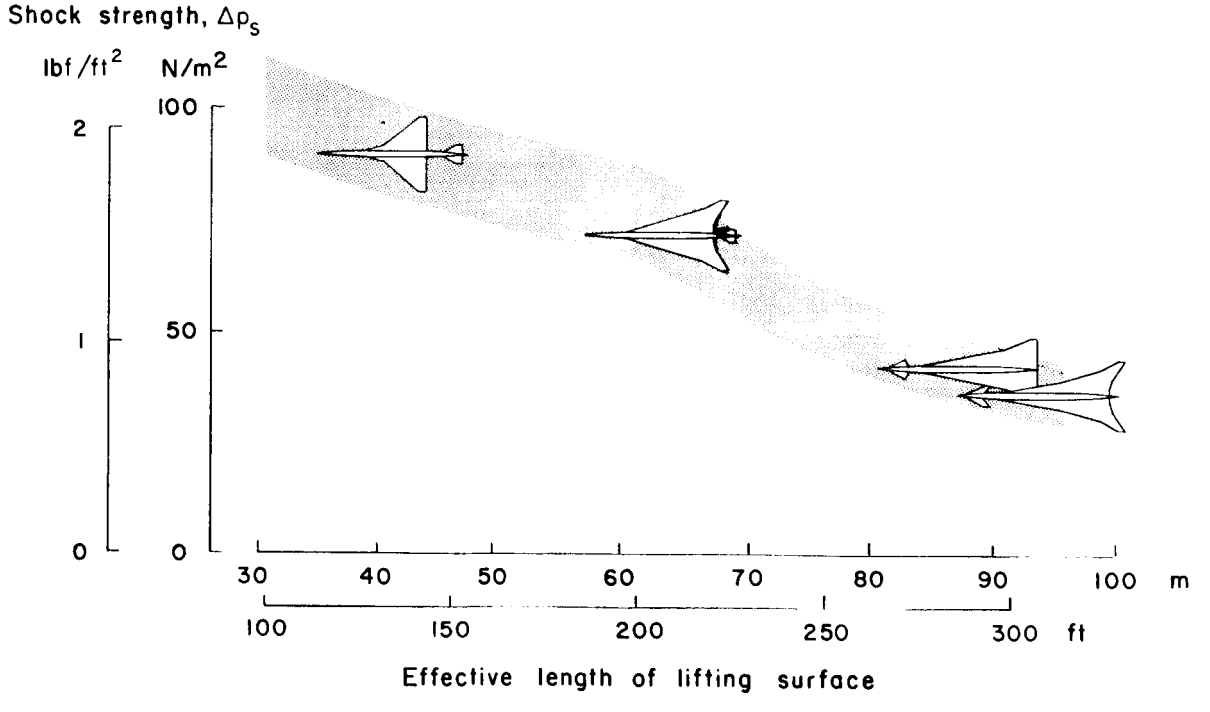


Figure 19.- Conceivable sonic-boom levels associated with departures from conventional design procedures. Speed, M = 2.7; range, 2500 n. mi.; payload, 234 passengers.

As noted previously, many design features conducive to sonic-boom minimization are in direct conflict with other aspects of airplane design. A comprehensive study of qualified airplane design teams is required to determine the extent to which sonic-boom minimization concepts can be effectively incorporated in practical and economically attractive airplanes.

## CONCLUDING REMARKS

An investigation of sonic-boom minimization concepts employed in the design of large (234 passenger) supersonic transport airplanes indicates that shock strengths of somewhat less than 48 newtons/meter$^2$ (1 pound force/foot$^2$) for a design range of 2500 nautical miles and a cruise Mach number of 2.7 are within the realm of possibility. An important design feature of such an airplane is a wing of large area and long root chord located well aft with respect to the fuselage. The wing would incorporate twist and camber designed to meet sonic-boom shaping, as well as drag minimization requirements, and would employ positive dihedral. A canard surface may also be utilized in optimization of the lift distribution for sonic-boom benefits. Because many of the design features are in direct contradiction to presently accepted design practices, further study by qualified airplane design teams is required to ascertain sonic-boom shock-strength levels actually attainable for practical supersonic transports.

Langley Research Center,
National Aeronautics and Space Administration,
Hampton, Va., April 10, 1973.

## REFERENCES


1. Carlson, H. W.; and Maglieri, D. J.: Review of Sonic-Boom Generation Theory and Prediction Methods. J. Acoust. Soc. Amer., vol. 51, no. 2, pt. 3, Feb. 1972, pp. 675-685.

2. Carlson, Harry W.; Mack, Robert J.; and Morris, Odell A.: Sonic-Boom Pressure-Field Estimation Techniques. J. Acoust. Soc. Amer., vol. 39, no. 5, pt. 2, May 1966, pp. S10-S18.

3. Whitham, G. B.: The Flow Pattern of a Supersonic Projectile. Commun. Pure Appl. Math., vol. V, no. 3, Aug. 1952, pp. 301-348.

4. Whitham, G. B.: On the Propagation of Weak Shock Waves. J. Fluid Mech., vol. 1, pt. 3, Sept. 1956, pp. 290-318.

5. Hayes, Wallace D.; Haefeli, Rudolph C.; and Kulsrud, H. E.: Sonic Boom Propagation in a Stratified Atmosphere, With Computer Program. NASA CR-1299, 1969.

6. Walkden, F.: The Shock Pattern of a Wing-Body Combination, Far From the Flight Path. Aeronaut. Quart., vol. IX, pt. 2, May 1958, pp. 164-194.

7. Hayes, Wallace D.: Linearized Supersonic Flow. Rep. No. AL-222, North Amer. Aviat., Inc., June 18, 1947.

8. Carlson, Harry W.: Correlation of Sonic-Boom Theory With Wind-Tunnel and Flight Measurements. NASA TR R-213, 1964.

9. Middleton, Wilbur D.; and Carlson, Harry W.: A Numerical Method for Calculating Near-Field Sonic-Boom Pressure Signatures. NASA TN D-3082, 1965.

10. Jones, L. B.: Lower Bounds for Sonic Bangs. J. Roy Aeronaut. Soc., vol. 65, no. 606, June 1961, pp. 433-436.

11. Carlson, Harry W.: Influence of Airplane Configuration on Sonic-Boom Characteristics. J. Aircraft, vol. 1, no. 2, Mar.-Apr. 1964, pp. 82-86.

12. McLean, F. Edward: Some Nonasymptotic Effects on the Sonic Boom of Large Airplanes. NASA TN D-2877, 1965.

13. McLean, F. Edward; and Shrout, Barrett L.: Design Methods for Minimization of Sonic-Boom Pressure-Field Disturbances. J. Acoust. Soc. Amer., vol. 39, no. 5, pt. 2, May 1966, pp. S19-S25.

14. McLean, F. Edward; Carlson, Harry W.; and Hunton, Lynn W.: Sonic-Boom Characteristics of Proposed Supersonic and Hypersonic Airplanes. NASA TN D-3587, 1966.

15. Carlson, Harry W.; Mack, Robert J.; and Morris, Odell A.: A Wind-Tunnel Investigation of the Effect of Body Shape on Sonic-Boom Pressure Distributions. NASA TN D-3106, 1965.

16. Carlson, Harry W.; McLean, F. Edward; and Shrout, Barrett L.: A Wind-Tunnel Study of Sonic-Boom Characteristics for Basic and Modified Models of a Supersonic Transport Configuration. NASA TM X-1236, 1966.

17. Barger, Raymond L.: Design of Bodies To Produce Specified Sonic-Boom Signatures. NASA TN D-4704, 1968.

18. Barger, Raymond L.; and Jordan, Frank L., Jr.: Investigation of a Class of Bodies That Generate Far-Field Sonic-Boom Shock Strength and Impulse Independent of Body Length and Volume. NASA TN D-5148, 1969.

19. Jones, L. B.: Lower Bounds for the Pressure Jumps of the Shock Waves of a Supersonic Transport of Given Length. Aeronaut. Quart., vol. XXIII, pt. 1, Feb. 1972, pp. 62-76.

20. George, A. R.: Lower Bounds for Sonic Booms in the Midfield. AIAA J., vol. 7, no. 8, Aug. 1969, pp. 1542-1545.

21. George, A. R.; and Seebass, R.: Sonic Boom Minimization Including Both Front and Rear Shocks. AIAA J., vol. 9, no. 10, Oct. 1971, pp. 2091-2093.

22. Seebass, R.; and George, A. R.: Sonic-Boom Minimization. J. Acoust. Soc. Amer., vol. 51, no. 2 (pt. 3), Feb. 1972, pp. 686-694.

23. von Gierke, H. E.; and Nixon, C. W.: Human Response to Sonic Boom in the Laboratory and the Community. J. Acoust. Soc. Amer., vol. 51, no. 2 (pt. 3), Feb. 1972, pp. 766-782.

24. Clarkson, Brian L.; and Mayes, William H.: Sonic-Boom-Induced Building Structure Responses Including Damage. J. Acoust. Soc. Amer., vol. 51, no. 2 (pt. 3), Feb. 1972, pp. 742-757.

25. Miller, David S.; and Carlson, Harry W.: Application of Heat and Force Fields to Sonic-Boom Minimization. J. Aircraft, vol. 8, no. 8, Aug. 1971, pp. 657-662.

26. Batdorf, S. B.: Alleviation of the Sonic Boom by Thermal Means. J. Aircraft, vol. 9, no. 2, Feb. 1972, pp. 150-156.

27. Lipfert, F. W.: An Analytical Study of Some Possible Sonic Boom Alleviation Schemes. AIAA Paper No. 72-653, June 1972.

28. Nichols, Mark R.; Keith, Arvid L., Jr.; and Foss, Willard E., Jr.: The Second-Generation Supersonic Transport. Vehicle Technology for Civil Aviation – The Seventies and Beyond, NASA SP-292, 1971, pp. 409-428.

29. Baals, Donald D.; Robins, A. Warner; and Harris, Roy V., Jr.: Aerodynamic Design Integration of Supersonic Aircraft. J. Aircraft, vol. 7, no. 5, Sept.-Oct. 1970, pp. 385-394.

30. Carlson, Harry W.; and Harris, Roy V., Jr.: A Unified System of Supersonic Aerodynamic Analysis. Analytic Methods in Aircraft Aerodynamics, NASA SP-228, 1970, pp. 639-658.

31. Polhamus, Edward C.: Application of the Leading-Edge-Suction Analogy of Vortex Lift to the Drag Due to Lift of Sharp-Edge Delta Wings. NASA TN D-4739, 1968.

32. Ferri, Antonio: Airplane Configurations for Low Sonic Boom. Third Conference on Sonic Boom Research, Ira R. Schwartz, ed., NASA SP-255, 1971, pp. 255-275.

33. Ferri, Antonio; and Schwartz, Ira R.: Sonic Boom Generation Propagation and Minimization. AIAA Paper No. 72-194, Jan. 1972.

34. Howell, Clarence S.; Sigalla, Armand; and Kane, Edward J.: Sonic Boom Considerations in Aircraft Design. Aircraft Engine Noise and Sonic Boom, AGARD CP No. 42, May 1969, pp. 30-1 – 30-7.

35. Craidon, Charlotte B.: Description of a Digital Computer Program for Airplane Configuration Plots. NASA TM X-2074, 1970.

36. Harris, Roy V., Jr.: An Analysis and Correlation of Aircraft Wave Drag. NASA TM X-947, 1964.

37. Carlson, Harry W.; and Middleton, Wilbur D.: A Numerical Method for the Design of Camber Surfaces of Supersonic Wings With Arbitrary Planforms. NASA TN D-2341, 1964.

38. Middleton, Wilbur D.; and Carlson, Harry W.: Numerical Method of Estimating and Optimizing Supersonic Aerodynamic Characteristics of Arbitrary Planform Wings. J. Aircraft, vol. 2, no. 4, July-Aug. 1965, pp. 261-265.

39. Shrout, Barrett L.: Extension of a Numerical Solution for the Aerodynamic Characteristics of a Wing To Include a Canard or Horizontal Tail. Paper presented at AGARD Specialists Meeting on Aerodynamic Interference (Silver Spring, Md.), Sept. 1970.

TABLE I.- NUMERICAL DESCRIPTION OF BASIC SST DESIGN CONCEPTS.

WAVE DRAG PROGRAM FORMAT (REF. 35)

(a) Conventional delta-wing SST

[Dimensions in m and $m^2$]

```
  1  1 -1  1  1  1      5 11  2 19 30 19 28                2  6  1  9  1  9
 773.32                                                                        REFA
 0.      10.     20.     30.     40.     50.     60.     70.     80.     90.   XAF10
 100.                                                                          XAF11
 28.194  1.981  0.000 34.168                                                   WAFORG1
 37.490  4.572  0.000 24.685                                                   WAFORG2
 43.891  9.754  0.000 17.678                                                   WAFORG3
 50.444 15.240  0.000 11.125                                                   WAFORG4
 58.217 21.641  0.000  3.353                                                   WAFORG5
  0.000  -.213  -.427  -.640  -.853 -1.067 -1.280 -1.494 -1.707 -1.920  TZORD1
 -2.134                                                                        TZ1
  0.000  -.154  -.308  -.462  -.617  -.771  -.925 -1.079 -1.233 -1.387  TZORD2
 -1.542                                                                        TZ2
  0.000  -.110  -.221  -.331  -.442  -.552  -.662  -.773  -.883  -.994  TZORD3
 -1.104                                                                        TZ3
  0.000  -.069  -.139  -.208  -.278  -.347  -.417  -.486  -.556  -.625  TZORD4
  -.695                                                                        TZ4
  0.000  -.021  -.042  -.063  -.084  -.105  -.126  -.147  -.168  -.188  TZORD5
  -.209                                                                        TZ5
 0.      .53     .94    1.24   1.43   1.5    1.43   1.24   .94     .53      WAFORD10
 0.                                                                           WAFORD11
 0.      .53     .94    1.24   1.43   1.5    1.43   1.24   .94     .53      WAFORD20
 0.                                                                           WAFORD21
 0.      .53     .94    1.24   1.43   1.5    1.43   1.24   .94     .53      WAFORD30
 0.                                                                           WAFORD31
 0.      .53     .94    1.24   1.43   1.5    1.43   1.24   .94     .53      WAFORD40
 0.                                                                           WAFORD41
 0.      .53     .94    1.24   1.43   1.5    1.43   1.24   .94     .53      WAFORD50
 0.                                                                           WAFORD51
  0.000  1.524  3.048  4.572  6.096  7.620  9.144 10.668 12.192 13.716  XFUS10
 15.240 16.764 18.288 19.812 21.336 22.860 24.384 25.908 27.432 28.956  XFUS11
 30.480 32.004 33.528 35.052 36.576 38.100 39.624 41.148 42.672 44.196  XFUS12
  0.000  0.000  0.000  0.000  0.000  0.000  0.000  0.000  0.000  0.000  ZFUS10
  0.000  0.000  0.000  0.000  0.000  0.000  0.000  -.030  -.122  -.197  ZFUS11
  -.285  -.373  -.462  -.550  -.639  -.727  -.815  -.903  -.992 -1.080  ZFUS12
  0.000   .465  1.068  1.858  2.769  3.716  4.664  5.621  6.578  7.525  FUSA10
  8.408  9.244  9.941 10.554 11.037 11.427 11.752 11.910 11.984 11.984  FUSA11
 11.966 11.929 11.892 11.845 11.752 11.724 11.706 11.687 11.687 11.687  FUSA12
 44.196 45.720 47.244 48.768 50.292 51.816 53.340 54.864 56.388 57.912  XFUS20
 59.436 60.960 62.484 64.008 65.532 67.056 68.580 70.104 71.628 73.152  XFUS21
 74.676 76.200 77.724 79.248 80.772 82.296 83.820 85.344                 XFUS22
 -1.080 -1.169 -1.257 -1.345 -1.434 -1.522 -1.611 -1.699 -1.787 -1.876  ZFUS20
 -1.964 -2.052 -2.134 -2.134 -2.134 -2.134 -2.134 -2.134 -2.134 -2.134  ZFUS21
 -2.134 -2.134 -2.134 -2.134 -2.134 -2.134 -2.134 -2.134                 ZFUS22
 11.687 11.641 11.594 11.520 11.390 11.241 11.037 10.777 10.498 10.191  FUSA20
  9.811  9.458  9.095  8.659  8.250  7.795  7.321  6.763  6.132  5.444  FUSA21
  4.673  3.883  3.103  2.341  1.635  1.022   .465  0.000                 FUSA22
 53.706  4.877 -3.048                                                   PODORG1
  0.000  3.048  6.096  7.620  9.144 11.278                             XPOD1
   .808   .930  1.052  1.113  1.036   .945                             PODR1
 53.706  9.754 -3.048                                                   PODORG2
  0.000  3.048  6.096  7.620  9.144 11.278                             XPOD2
   .808   .930  1.052  1.113  1.036   .945                             PODR2
 65.380  0.000  -.914 14.478 75.286  0.000  6.401  3.200               FINORG
 0.      10.     25.     40.     50.     60.     75.     90.     100.    XFIN
 0.      .53    1.11    1.43    1.5    1.43    1.11    .53     0.      FINORD
 71.628   .914 -2.134 10.516 75.248  5.182 -2.134  2.438               CANORG
 0.      10.     25.     40.     50.     60.     75.     90.     100.    XCAN
 0.      .53    1.11    1.43    1.5    1.43    1.11    .53     0.      CANORD
```

TABLE 1.- NUMERICAL DESCRIPTION OF BASIC SST DESIGN CONCEPTS.

WAVE DRAG PROGRAM FORMAT (REF. 35) – Continued

(b) Conventional arrow-wing SST

[Dimensions in m and $m^2$]

```
  1  1 -1  1  1  1      5 12  1 19 30                        2  6  2 10  1 10
 982.45                                                                        REFA
0.      5.      10.     20.     30.     40.     50.     60.     70.     80.    XAF10
90.     100.                                                                  XAF12
 24.994  1.829  0.000 48.768                                                   WAFORG1
 35.052  4.877  0.000 38.710                                                   WAFORG2
 52.121  9.754  0.000 23.043                                                   WAFORG3
 69.037 14.630  0.000  9.754                                                   WAFORG4
 78.334 20.117  0.000  4.328                                                   WAFORG5
  0.000  -.168  -.335  -.671 -1.006 -1.341 -1.676 -2.012 -2.347 -2.682  TZORD10
-3.018 -3.353                                                                TZ12
  0.000  -.133  -.266  -.532  -.798 -1.065 -1.331 -1.597 -1.863 -2.129  TZORD20
-2.395 -2.661                                                                TZ22
  0.000  -.079  -.158  -.317  -.475  -.634  -.792  -.951 -1.109 -1.267  TZORD30
-1.429 -1.584                                                                TZ32
  0.000  -.034  -.067  -.134  -.201  -.268  -.335  -.402  -.469  -.536  TZORD40
 -.604  -.671                                                                TZ42
  0.000  -.015  -.030  -.059  -.089  -.119  -.149  -.179  -.208  -.238  TZORD50
 -.268  -.297                                                                TZ52
0.      .575    .78    1.03   1.17   1.26   1.3    1.24   1.08    .82      WAFORD10
.45     0.                                                                   WAFORD12
0.      .575    .78    1.03   1.17   1.26   1.3    1.24   1.08    .82      WAFORD20
.45     0.                                                                   WAFORD22
0.      .575    .78    1.03   1.17   1.26   1.3    1.24   1.08    .82      WAFORD30
.45     0.                                                                   WAFORD32
0.      .575    .78    1.03   1.17   1.26   1.3    1.24   1.08    .82      WAFORD40
.45     0.                                                                   WAFORD42
0.      .575    .78    1.03   1.17   1.26   1.3    1.24   1.08    .82      WAFORD50
.45     0.                                                                   WAFORD52
  0.000  3.048  6.096  9.144 12.192 15.240 18.288 21.336 24.384 27.432  XFUS10
 30.480 33.528 36.576 39.624 42.672 45.720 48.768 51.816 54.864 57.912  XFUS20
 60.960 64.008 67.056 70.104 73.152 76.200 79.248 82.296 86.868 89.916  XFUS30
  0.000  0.000  0.000  0.000  0.000  0.000  0.000  0.000  0.000  -.213  ZFUS10
 -.427  -.640  -.853 -1.067 -1.280 -1.493 -1.646 -1.829 -2.042 -2.225  ZFUS20
-2.438 -2.621 -2.804 -3.078 -3.261 -3.353 -3.353 -3.353 -3.353 -3.353  ZFUS30
  0.000  1.115  2.880  4.738  6.503  8.268  9.848 11.241 11.613 11.474  FUSA10
 10.870 10.312  9.848  9.755  9.848  9.894  9.941  9.941  9.348  9.708  FUSA20
  9.476  9.012  8.547  7.711  6.689  5.481  4.088  2.555   .557  0.000  FUSA30
 84.922  4.877 -3.962                                                   PODORG1
  0.000  3.048  6.096  7.620  9.144 11.278                              XPOD1
  .808   .930  1.052  1.113  1.036   .945                              PODR1
 60.142  9.754 -2.743                                                   PODORG2
  0.000  3.048  6.096  7.620  9.144 11.278                              XPOD2
  .808   .930  1.052  1.113  1.036   .945                              PODR2
 81.991  0.000 -3.048  6.858 85.649  0.000   .610  2.438                FINORG1
0.      5.      10.     20.     40.     50.     60.     70.     80.    100.   XFIN1
0.      .575    .78    1.03   1.26   1.3    1.24   1.08    .82     0.       FINORD1
 69.037 14.630  -.305 11.278 79.705 14.630  3.048  1.676                   FINORG2
0.      5.      10.     20.     40.     50.     60.     70.     80.    100.   XFIN2
0.      .575    .78    1.03   1.26   1.3    1.24   1.08    .82     0.       FINORD2
 79.553   .610 -3.353  7.620 84.125  3.353 -3.353  2.743                   CANORG
0.      5.      10.     20.     40.     50.     60.     70.     80.    100.   XCAN
0.      .575    .78    1.03   1.26   1.3    1.24   1.08    .82     0.       CANORD
```

TABLE 1.- NUMERICAL DESCRIPTION OF BASIC SST DESIGN CONCEPTS.

WAVE DRAG PROGRAM FORMAT (REF. 35) – Continued

(c) Aft delta-wing SST

[Dimensions in m and $m^2$]

```
  1  1 -1  1  1  1     3 12  1 19 30                    2  6  1 10  1 10
1135.65                                                                    REFA
C.      5.      10.     20.     30.     40.     50.     60.     70.     80.  XAF10
90.     100.                                                               XAF12
 25.908  1.524  0.000 65.532                                               WAFORG1
 73.762 10.973  0.000 17.678                                               WAFORG2
 88.697 17.678  0.000  2.743                                               WAFORG3
  0.000  -.168  -.335  -.671 -1.006 -1.341 -1.676 -2.012 -2.347 -2.682  TZORD10
 -3.018 -3.353                                                           TZ12
  0.000  -.045  -.091  -.181  -.271  -.362  -.452  -.543  -.633  -.724  TZORD 20
  -.814  -.904                                                           TZ 22
  0.000  -.007  -.014  -.028  -.042  -.056  -.070  -.084  -.098  -.112  TZORD 30
  -.126  -.140                                                           TZ 32
0.      .47     .65     .84     .94     1.      1.      .93     .79     .58  WAFORD10
.32     0.                                                               WAFORD12
0.      .47     .65     .84     .94     1.      1.      .93     .79     .58  WAFORD20
.32     0.                                                               WAFORD22
0.      .47     .65     .84     .94     1.      1.      .93     .79     .58  WAFORD30
.32     0.                                                               WAFORD32
  0.000  3.048  6.096  9.144 12.192 15.240 18.288 21.336 24.384 27.432  XFUS10
 30.480 33.528 36.576 39.624 42.672 45.720 48.768 51.816 54.864 57.912  XFUS20
 60.960 64.008 67.056 70.104 73.152 76.200 79.248 82.296 86.868 91.440  XFUS30
  0.000  0.000  0.000  0.000  0.000  0.000  0.000  0.000  0.000  0.000  ZFUS10
  -.158  -.320  -.479  -.640  -.799  -.957 -1.119 -1.277 -1.436 -1.597  ZFUS20
 -1.756 -1.917 -2.076 -2.234 -2.396 -2.554 -2.713 -2.874 -3.112 -3.353  ZFUS30
  0.000  .650  1.858  3.345  4.924  6.503  7.990  9.383 10.591 11.706  FUSA10
 12.356 12.728 12.728 12.356 11.799 11.148 10.684 10.405 10.034  9.755  FUSA20
  9.569  9.290  8.733  7.990  6.968  5.760  4.366  2.787   .836  0.000  FUSA30
 82.601  4.877 -3.353                                                   PODORG1
  0.000  3.048  6.096  7.620  9.144 11.278                             XPOD1
   .808   .930  1.052  1.113  1.036   .945                             PODR1
 82.601  9.754 -2.438                                                   PODORG2
  0.000  3.048  6.096  7.620  9.144 11.278                             XPOD2
   .808   .930  1.052  1.113  1.036   .945                             PODR2
 76.352  0.000 -1.829 13.411 85.344  0.000  5.486  3.048                FINORG
0.      5.      10.     20.     30.     40.     50.     60.     80.    100.  XFIN
0.      .47     .65     .85     .94     1.      1.      .93     .59    0.    FINORD
  6.706  1.219  0.000 10.973 14.813  6.096  0.000  0.000                  CANORG
0.      5.      10.     20.     30.     40.     50.     60.     80.    100.  XCAN
0.      .47     .65     .85     .94     1.      1.      .93     .59    0.    CANORD
```

TABLE 1.- NUMERICAL DESCRIPTION OF BASIC SST DESIGN CONCEPTS.

WAVE DRAG PROGRAM FORMAT (REF. 35) – Concluded

(d) Aft arrow-wing SST

[Dimensions in m and $m^2$]

```
  1  1 -1  1  1  1     6 12  1 19 30                    2  6  1  9  1  5
1156.32                                                                    REFA
0.0     5.0    10.0   20.0   30.0   40.0   50.0   60.0   70.0   80.0      XAF 10
90.0   100.0                                                               XAF 12
 19.812  1.829  0.000 67.361                                               WAFORG 1
 40.813  4.877  0.000 46.360                                               WAFORG 2
 57.607  7.315  0.000 30.328                                               WAFORG 3
 65.928  9.754  0.000 22.769                                               WAFORG 4
 82.601 14.630  0.000  9.540                                               WAFORG 5
 91.745 20.117  0.000  4.267                                               WAFORG 6
  0.000  -.125  -.250  -.500  -.750 -1.000 -1.250 -1.500 -1.750 -1.999     TZORD 10
-2.249 -2.499                                                              TZ 12
   .305   .219   .134  -.040  -.210  -.384  -.555  -.728  -.859 -1.070     TZORD 20
-1.244 -1.414                                                              TZ 22
   .305   .250   .192   .079  -.034  -.146  -.259  -.372  -.482  -.594     TZORD 30
 -.707  -.820                                                              TZ 32
   .305   .262   .219   .137   .052  -.054  -.119  -.201  -.287  -.372     TZORD 40
 -.454  -.539                                                              TZ 42
   .305   .287   .266   .235   .198   .165   .128   .091   .058   .021     TZORD 50
 -.015  -.049                                                              TZ 52
   .305   .296   .290   .274   .256   .241   .226   .210   .193   .177     TZORD 60
   .162   .146                                                            TZ 62
0.0     .47    .65    .87   1.01   1.07   1.08   1.02    .88    .67       WAFORD10
.37    0.0                                                               WAFORD12
0.0     .47    .65    .87   1.01   1.07   1.08   1.02    .88    .67       WAFORD20
.37    0.0                                                               WAFORD22
0.0     .47    .65    .87   1.01   1.07   1.08   1.02    .88    .67       WAFORD30
.37    0.0                                                               WAFORD32
0.0     .47    .65    .87   1.01   1.07   1.08   1.02    .88    .67       WAFORD40
.37    0.0                                                               WAFORD42
0.0     .47    .65    .87   1.01   1.07   1.08   1.02    .88    .67       WAFORD50
.37    0.0                                                               WAFORD52
0.0     .47    .65    .87   1.01   1.07   1.08   1.02    .88    .67       WAFORD60
.37    0.0                                                               WAFORD62
  0.000  3.048  6.096  9.144 12.192 15.240 18.288 21.336 24.384 27.432    XFUS 10
 30.480 33.528 36.576 39.624 42.672 45.720 48.768 51.816 54.864 57.912    XFUS 20
 60.960 64.008 67.056 70.104 73.152 76.200 79.248 82.296 85.344 91.440    XFUS 30
  0.000  0.000  0.000  0.000  0.000  0.000  0.000  -.064  -.195  -.323     ZFUS 10
 -.454  -.582  -.713  -.844  -.972 -1.103 -1.241 -1.362 -1.490 -1.622     ZFUS 20
-1.750 -1.881 -2.012 -2.140 -2.271 -2.399 -2.530 -2.658 -2.789 -3.048     ZFUS 30
  0.000  1.022  2.691  4.274  6.002  7.618  9.197 10.498 11.334 11.892    FUSA 10
 11.892 11.706 11.334 10.870 10.498 10.219  9.541  9.662  9.476  9.197    FUSA 20
  9.012  8.640  8.083  7.432  6.595  5.295  3.902  2.508  1.208  0.000    FUSA 30
 78.334  4.877 -2.743                                                     PODORG 1
  0.000  3.048  6.096  7.620  9.144 11.278                               XPOD 1
   .606   .930  1.052  1.113  1.036   .945                               PODR 1
 79.898  9.754 -1.829                                                     PODORG 2
  0.000  3.048  6.096  7.620  9.144 11.278                               XPOD 2
   .606   .930  1.052  1.113  1.036   .945                               PODR 2
 82.601 14.630   .305  9.754 93.878 14.630  5.182  1.524                 FINORG
0.0     5.0    15.0   30.0   40.0   50.0   60.0   75.0  100.0            XFIN
0.0     .47    .77   1.01   1.07   1.08   1.02    .78    0.0             FINORD
  3.048  1.219  0.000  9.876 16.764  5.486  0.000  1.524                 CANORG
0.0     5.0    15.0   30.0   40.0   50.0   60.0   75.0  100.0            XCAN
0.0     .47    .77   1.01   1.07   1.08   1.02    .78    0.0             CANORD
```

TABLE 2.- CAMBER SURFACE ORDINATES $(z - z_{LE}, m)$ FOR BASIC SST DESIGN CONCEPTS

(a) Conventional delta-wing SST; $C_{L,design} = 0.038$

| $\frac{y}{b/2}$ | $\frac{x - x_{LE}}{c}$ 0.0000 | .1000 | .2000 | .3000 | .4000 | .5000 | .6000 | .7000 | .8000 | .9000 | 1.0000 |
|---|---|---|---|---|---|---|---|---|---|---|---|
| 0.0000 | 0.0000 | -.1149 | -.2509 | -.4006 | -.5606 | -.7266 | -.8949 | -1.0619 | -1.2229 | -1.3753 | -1.5172 |
| .0200 | 0.0000 | -.1142 | -.2473 | -.3946 | -.5524 | -.7164 | -.8824 | -1.0472 | -1.2060 | -1.3563 | -1.4963 |
| .0400 | 0.0000 | -.1119 | -.2413 | -.3869 | -.5425 | -.7043 | -.8685 | -1.0308 | -1.1875 | -1.3359 | -1.4743 |
| .0800 | 0.0000 | -.1045 | -.2499 | -.4137 | -.5868 | -.7645 | -.9422 | -1.1153 | -1.2816 | -1.4390 | -1.5858 |
| .1400 | 0.0000 | -.0109 | -.0622 | -.1340 | -.2163 | -.3031 | -.3914 | -.4798 | -.5675 | -.6534 | -.7367 |
| .2200 | 0.0000 | .0026 | .0085 | .0102 | .0082 | .0030 | -.0051 | -.0158 | -.0287 | -.0435 | -.0600 |
| .2800 | 0.0000 | -.0500 | -.0835 | -.1165 | -.1495 | -.1830 | -.2172 | -.2517 | -.2865 | -.3215 | -.3565 |
| .3600 | 0.0000 | -.0516 | -.0976 | -.1365 | -.1726 | -.2078 | -.2424 | -.2766 | -.3107 | -.3443 | -.3777 |
| .4600 | 0.0000 | -.0470 | -.0893 | -.1310 | -.1669 | -.2035 | -.2359 | -.2674 | -.2980 | -.3280 | -.3573 |
| .5600 | 0.0000 | -.0333 | -.0703 | -.1060 | -.1408 | -.1747 | -.2069 | -.2369 | -.2648 | -.2919 | -.3179 |
| .6600 | 0.0000 | -.0353 | -.0667 | -.0958 | -.1252 | -.1539 | -.1817 | -.2092 | -.2357 | -.2615 | -.2861 |
| .7600 | 0.0000 | -.0252 | -.0463 | -.0699 | -.0936 | -.1161 | -.1384 | -.1605 | -.1822 | -.2033 | -.2242 |
| .8600 | 0.0000 | -.0190 | -.0378 | -.0560 | -.0732 | -.0900 | -.1066 | -.1233 | -.1398 | -.1559 | -.1718 |
| 1.0000 | 0.0000 | -.0098 | -.0195 | -.0272 | -.0337 | -.0401 | -.0460 | -.0512 | -.0563 | -.0614 | -.0659 |

TABLE 2.- CAMBER SURFACE ORDINATES $(z - z_{LE}, m)$ FOR BASIC SST DESIGN CONCEPTS – Continued

(b) Conventional arrow-wing SST; $C_{L,design} = 0.061$

| $\frac{y}{b/2}$ | $\frac{x - x_{LE}}{c}$ 0.0000 | .1000 | .2000 | .3000 | .4000 | .5000 | .6000 | .7000 | .8000 | .9000 | 1.0000 |
|---|---|---|---|---|---|---|---|---|---|---|---|
| 0.0000 | 0.0000 | -.3458 | -.7493 | -1.1828 | -1.6186 | -2.0355 | -2.4184 | -2.7556 | -3.0379 | -3.2575 | -3.4079 |
| .0400 | 0.0000 | -.3293 | -.7196 | -1.1422 | -1.5684 | -1.9774 | -2.3541 | -2.6871 | -2.9671 | -3.1866 | -3.3392 |
| .0800 | 0.0000 | -.2986 | -.7048 | -1.1435 | -1.5834 | -2.0043 | -2.3918 | -2.7352 | -3.0253 | -3.2552 | -3.4189 |
| .1400 | 0.0000 | -.0731 | -.2946 | -.5623 | -.8499 | -1.1413 | -1.4249 | -1.6925 | -1.9366 | -2.1520 | -2.3335 |
| .2200 | 0.0000 | -.0066 | -.1241 | -.2868 | -.4746 | -.6750 | -.8796 | -1.0824 | -1.2783 | -1.4633 | -1.6338 |
| .3000 | 0.0000 | .0527 | -.0087 | -.1114 | -.2385 | -.3803 | -.5306 | -.6851 | -.8398 | -.9920 | -1.1391 |
| .3800 | 0.0000 | .0471 | .0237 | -.0383 | -.1227 | -.2215 | -.3299 | -.4449 | -.5638 | -.6843 | -.8047 |
| .4600 | 0.0000 | .0819 | .0604 | .0494 | -.0003 | -.0636 | -.1361 | -.2159 | -.3009 | -.3895 | -.4805 |
| .5400 | 0.0000 | .0612 | .0735 | .0633 | .0373 | .0002 | -.0450 | -.0971 | -.1546 | -.2163 | -.2813 |
| .6200 | 0.0000 | .0742 | .1027 | .1093 | .1017 | .0851 | .0623 | .0332 | -.0006 | -.0379 | -.0776 |
| .7200 | 0.0000 | .0304 | .0733 | .1007 | .1256 | .1465 | .1651 | .1815 | .1959 | .2088 | .2199 |
| .7400 | 0.0000 | .0036 | .0328 | .0512 | .0673 | .0819 | .0936 | .1047 | .1140 | .1219 | .1288 |
| .8400 | 0.0000 | -.0201 | -.0393 | -.0566 | -.0661 | -.0764 | -.0872 | -.0978 | -.1084 | -.1195 | -.1308 |
| .9200 | 0.0000 | -.0295 | -.0421 | -.0568 | -.0745 | -.0898 | -.1041 | -.1164 | -.1288 | -.1414 | -.1531 |
| 1.0000 | 0.0000 | -.0244 | -.0470 | -.0553 | -.0636 | -.0678 | -.0712 | -.0727 | -.0728 | -.0721 | -.0694 |

TABLE 2.- CAMBER SURFACE ORDINATES $(z - z_{LE}, m)$ FOR BASIC SST DESIGN CONCEPTS – Continued

(c) Aft delta-wing SST; $C_{L,design} = 0.03$

| $\frac{y}{b/2}$ | $\frac{x-x_{LE}}{c}$ 0.0000 | .1000 | .2000 | .3000 | .4000 | .5000 | .6000 | .7000 | .8000 | .9000 | 1.0000 |
|---|---|---|---|---|---|---|---|---|---|---|---|
| 0.0000 | 0.0000 | -.2442 | -.5430 | -.8643 | -1.2402 | -1.5910 | -1.9213 | -2.2197 | -2.4765 | -2.6841 | -2.8354 |
| .0400 | 0.0000 | -.2484 | -.5557 | -.9012 | -1.2564 | -1.6004 | -1.9185 | -2.1985 | -2.4312 | -2.6088 | -2.7242 |
| .0800 | 0.0000 | -.2539 | -.6026 | -.9872 | -1.3755 | -1.7459 | -2.0851 | -2.3752 | -2.6130 | -2.7885 | -2.8951 |
| .1200 | 0.0000 | -.1502 | -.4654 | -.8240 | -1.1908 | -1.5450 | -1.8724 | -2.1619 | -2.4046 | -2.5936 | -2.7227 |
| .1800 | 0.0000 | .0240 | -.1194 | -.3203 | -.5484 | -.7869 | -1.0242 | -1.2518 | -1.4624 | -1.6507 | -1.8115 |
| .2400 | 0.0000 | .0785 | .0029 | -.1292 | -.2926 | -.4716 | -.6585 | -.8460 | -1.0282 | -1.2009 | -1.3630 |
| .3000 | 0.0000 | .1048 | .0715 | -.0143 | -.1305 | -.2659 | -.4128 | -.5654 | -.7193 | -.8710 | -1.0172 |
| .3600 | 0.0000 | .1163 | .1133 | .0624 | -.0179 | -.1170 | -.2294 | -.3501 | -.4759 | -.6038 | -.7300 |
| .4200 | 0.0000 | .1193 | .1383 | .1139 | .0653 | -.0053 | -.0872 | -.1786 | -.2767 | -.3761 | -.4801 |
| .4800 | 0.0000 | .1167 | .1499 | .1466 | .1206 | .0779 | .0230 | -.0413 | -.1108 | -.1837 | -.2585 |
| .5400 | 0.0000 | .1106 | .1524 | .1642 | .1573 | .1365 | .1074 | .0727 | .0336 | -.0089 | -.0599 |
| .6000 | 0.0000 | .0956 | .1431 | .1721 | .1917 | .2050 | .2132 | .2170 | .2169 | .2132 | .2065 |
| .6200 | 0.0000 | .0906 | .1651 | .2291 | .2853 | .3351 | .3794 | .4185 | .4529 | .4830 | .5090 |
| .6400 | 0.0000 | .0453 | .0827 | .1121 | .1355 | .1551 | .1704 | .1824 | .1913 | .1975 | .2012 |
| .7000 | 0.0000 | .0112 | .0249 | .0331 | .0375 | .0393 | .0389 | .0367 | .0328 | .0272 | .0203 |
| .8000 | 0.0000 | -.0038 | -.0062 | .0012 | .0001 | -.0019 | -.0051 | -.0092 | -.0142 | -.0200 | -.0264 |
| .9000 | 0.0000 | -.0051 | -.0080 | -.0087 | -.0097 | -.0119 | -.0142 | -.0167 | -.0201 | -.0233 | -.0270 |
| 1.0000 | 0.0000 | -.0062 | -.0125 | -.0130 | -.0117 | -.0105 | -.0081 | -.0049 | -.0017 | .0018 | .0066 |

TABLE 2.- CAMBER SURFACE ORDINATES $(z - z_{LE}, m)$ FOR BASIC SST DESIGN CONCEPTS – Concluded

(d) Aft arrow-wing SST; $C_{L,design} = 0.03$

| $\frac{y}{b/2}$ | $\frac{x-x_{LE}}{c}$ = 0.0000 | .1000 | .2000 | .3000 | .4000 | .5000 | .6000 | .7000 | .8000 | .9000 | 1.0000 |
|---|---|---|---|---|---|---|---|---|---|---|---|
| 0.0000 | 0.0000 | -.3023 | -.7168 | -1.2078 | -1.7293 | -2.2489 | -2.7430 | -3.1932 | -3.5845 | -3.9038 | -4.1365 |
| .0200 | 0.0000 | -.3074 | -.7225 | -1.2014 | -1.6960 | -2.1766 | -2.6164 | -2.9980 | -3.3065 | -3.5286 | -3.6499 |
| .0400 | 0.0000 | -.3409 | -.8036 | -1.3215 | -1.8443 | -2.3382 | -2.7792 | -3.1486 | -3.4315 | -3.6146 | -3.6834 |
| .0600 | 0.0000 | -.3267 | -.8160 | -1.3587 | -1.9000 | -2.4056 | -2.8511 | -3.2178 | -3.4913 | -3.6578 | -3.7035 |
| .0800 | 0.0000 | -.2957 | -.8433 | -1.4381 | -2.0211 | -2.5574 | -3.0235 | -3.4017 | -3.6769 | -3.8362 | -3.8666 |
| .1000 | 0.0000 | -.0465 | -.3580 | -.7495 | -1.1656 | -1.5756 | -1.9582 | -2.2974 | -2.5799 | -2.7925 | -2.9252 |
| .1200 | 0.0000 | .0536 | -.1634 | -.4669 | -.8068 | -1.1554 | -1.4930 | -1.8051 | -2.0798 | -2.3047 | -2.4711 |
| .1600 | 0.0000 | .1369 | .0271 | -.1715 | -.4161 | -.6819 | -.9542 | -1.2204 | -1.4689 | -1.6908 | -1.8796 |
| .2000 | 0.0000 | .1770 | .1324 | .0016 | -.1756 | -.3806 | -.5998 | -.8218 | -1.0370 | -1.2391 | -1.4234 |
| .2400 | 0.0000 | .1978 | .1976 | .1187 | -.0072 | -.1617 | -.3329 | -.5103 | -.6876 | -.8606 | -1.0253 |
| .2800 | 0.0000 | .2137 | .2441 | .2030 | .1189 | .0086 | -.1159 | -.2487 | -.3860 | -.5246 | -.6620 |
| .3600 | 0.0000 | .1936 | .3130 | .3953 | .4518 | .4877 | .5063 | .5095 | .4991 | .4763 | .4424 |
| .4400 | 0.0000 | .0811 | .1126 | .1245 | .1230 | .1113 | .0922 | .0665 | .0358 | .0008 | -.0376 |
| .5200 | 0.0000 | .0514 | .0749 | .0846 | .0848 | .0776 | .0651 | .0482 | .0276 | .0040 | -.0220 |
| .6000 | 0.0000 | .0526 | .0775 | .0897 | .0949 | .0941 | .0897 | .0820 | .0712 | .0582 | .0434 |
| .6800 | 0.0000 | .0273 | .0526 | .0654 | .0738 | .0786 | .0803 | .0807 | .0798 | .0780 | .0753 |
| .7200 | 0.0000 | .0234 | .0517 | .0716 | .0987 | .1045 | .1191 | .1325 | .1449 | .1565 | .1672 |
| .7600 | 0.0000 | -.0046 | .0048 | .0108 | .0158 | .0208 | .0250 | .0288 | .0323 | .0353 | .0379 |
| .8000 | 0.0000 | -.0023 | -.0043 | -.0054 | -.0047 | -.0045 | -.0046 | -.0048 | -.0050 | -.0056 | -.0062 |
| .9000 | 0.0000 | -.0112 | -.0211 | -.0283 | -.0339 | -.0389 | -.0432 | -.0470 | -.0503 | -.0534 | -.0566 |
| 1.0000 | 0.0000 | -.0103 | -.0182 | -.0215 | -.0248 | -.0255 | -.0262 | -.0258 | -.0247 | -.0233 | -.0208 |

TABLE 3.- SUMMARY OF GEOMETRIC REFERENCE PARAMETERS FOR BASIC SST DESIGN CONCEPTS

| Parameter | Conventional delta | Conventional arrow | Aft delta | Aft arrow |
|---|---|---|---|---|
| Wing span, m (ft) . . . . . | 43.3 (142.0) | 40.2 (132.0) | 35.4 (116.0) | 40.2 (132.0) |
| Wing area, $m^2$ ($ft^2$) . . . . . | 773.3 (8324.0) | 982.4 (10 575.0) | 1135.6 (12 224.0) | 1158.3 (12 468.0) |
| Mean aerodynamic chord, m (ft) . . . | 22.7 (74.6) | 34.0 (111.4) | 45.4 (149.1) | 43.8 (143.7) |
| Aspect ratio . . . . . | 2.42 | 1.65 | 1.10 | 1.40 |
| Thickness ratio . . . . . | 0.030 | 0.026 | 0.020 | 0.022 |
| Fuselage length, m (ft) . . . . . | 85.3 (280.0) | 89.9 (295.0) | 91.4 (300.0) | 91.4 (300.0) |
| Center of gravity, m (ft) . . . . . | 50.0 (164.0) | 56.1 (184.0) | 63.7 (209.0) | 64.6 (212.0) |

TABLE 4.- WEIGHT AND BALANCE ESTIMATES FOR ASSUMED DESIGN GROSS WEIGHT OF 272 000 kg (600 000 lbm)

(a) Delta-wing configuration

| | Weight | | Center of gravity | |
|---|---|---|---|---|
| | kg | lbm | m | ft |
| Wing | 32 900 | 72 532 | 53.3 | 175.0 |
| Fuselage | 18 867 | 41 594 | 41.1 | 135.0 |
| Horizontal tail | 2 500 | 5 511 | 79.2 | 260.0 |
| Vertical tail | 2 489 | 5 488 | 75.6 | 247.9 |
| Controls | 4 300 | 9 480 | 59.3 | 194.7 |
| Landing gear | 11 473 | 25 305 | 48.2 | 158.0 |
| Propulsion system | 31 305 | 69 005 | 59.8 | 196.3 |
| Furnishings and equipment | 11 078 | 24 422 | 38.3 | 125.5 |
| Airplane systems | 9 044 | 19 939 | 38.3 | 125.5 |
| Empty airplane | 123 956 | 273 276 | 51.4 | 168.5 |
| Passengers (234) | 17 513 | 38 610 | 39.6 | 130.0 |
| Cargo and containers | 4 826 | 10 640 | 50.8 | 166.7 |
| Crew | 720 | 1 585 | 28.5 | 93.4 |
| Services | 4 157 | 9 165 | 42.9 | 140.7 |
| Passengers, cargo and containers, crew, and services | 27 216 | 60 000 | 41.8 | 137.2 |
| Loaded airplane without fuel | 151 171 | 333 276 | 49.7 | 162.9 |

TABLE 4.- WEIGHT AND BALANCE ESTIMATES FOR ASSUMED DESIGN GROSS WEIGHT OF 272 000 kg (600 000 lbm) – Continued

(b) Arrow-wing configuration

| | Weight | | Center of gravity | |
|---|---|---|---|---|
| | kg | lbm | m | ft |
| Wing | 37 658 | 83 022 | 61.0 | 200.0 |
| Fuselage | 19 761 | 43 565 | 42.2 | 138.3 |
| Horizontal tail | 1 625 | 3 582 | 84.8 | 278.3 |
| Vertical tail | 1 780 | 3 924 | 80.8 | 265.0 |
| Controls | 4 300 | 9 480 | 66.4 | 217.7 |
| Landing gear | 11 976 | 26 403 | 53.1 | 174.1 |
| Propulsion system | 32 682 | 72 052 | 71.9 | 236.0 |
| Furnishings and equipment | 11 078 | 24 422 | 40.9 | 134.1 |
| Airplane systems | 9 055 | 19 963 | 49.5 | 162.5 |
| Empty airplane | 129 915 | 286 413 | 58.4 | 191.5 |
| Passengers (234) | 17 513 | 38 610 | 40.6 | 133.3 |
| Cargo and containers | 4 844 | 10 680 | 51.8 | 170.0 |
| Crew | 720 | 1 585 | 31.5 | 103.3 |
| Services | 4 139 | 9 125 | 47.7 | 156.5 |
| Passengers, cargo and containers, crew, and services | 27 216 | 60 000 | 43.5 | 142.6 |
| Loaded airplane without fuel | 157 130 | 346 413 | 55.8 | 183.0 |

TABLE 4.- WEIGHT AND BALANCE ESTIMATES FOR ASSUMED DESIGN GROSS WEIGHT OF 272 000 kg (600 000 lbm) – Continued

(c) Aft delta-wing configuration

| | Weight | | Center of gravity | |
|---|---|---|---|---|
| | kg | lbm | m | ft |
| Wing | 35 503 | 78 270 | 71.6 | 235.0 |
| Fuselage | 19 559 | 43 121 | 44.2 | 145.0 |
| Canard | 2 638 | 5 815 | 13.7 | 45.0 |
| Vertical tail | 1 905 | 4 200 | 86.4 | 283.3 |
| Controls | 4 300 | 9 480 | 60.2 | 197.5 |
| Landing gear | 12 969 | 28 591 | 65.6 | 215.2 |
| Propulsion system | 32 346 | 71 311 | 89.6 | 294.0 |
| Furnishings and equipment | 11 078 | 24 422 | 44.0 | 144.5 |
| Airplane systems | 9 037 | 19 924 | 45.8 | 150.2 |
| Empty airplane | 129 335 | 285 134 | 65.8 | 216.0 |
| Passengers (234) | 17 513 | 38 610 | 44.2 | 145.0 |
| Cargo and containers | 4 844 | 10 680 | 55.8 | 183.0 |
| Crew | 720 | 1 585 | 32.1 | 105.2 |
| Services | 4 139 | 9 125 | 57.3 | 188.0 |
| Passengers, cargo and containers, crew, and services | 27 216 | 60 000 | 47.9 | 157.2 |
| Loaded airplane without fuel | 156 550 | 345 134 | 62.7 | 205.8 |

TABLE 4.- WEIGHT AND BALANCE ESTIMATES FOR ASSUMED DESIGN GROSS WEIGHT OF 272 000 kg (600 000 lbm) – Concluded

(d) Aft arrow-wing configuration

| | Weight | | Center of gravity | |
|---|---|---|---|---|
| | kg | lbm | m | ft |
| Wing | 39 993 | 88 169 | 73.2 | 240.0 |
| Fuselage | 18 817 | 41 484 | 43.4 | 142.5 |
| Canard | 2 961 | 6 527 | 13.7 | 45.0 |
| Vertical tail | 2 547 | 5 615 | 89.9 | 295.0 |
| Controls | 4 300 | 9 480 | 79.5 | 260.7 |
| Landing gear | 11 784 | 25 980 | 69.6 | 228.4 |
| Propulsion system | 32 520 | 71 695 | 86.0 | 282.3 |
| Furnishings and equipment | 11 078 | 24 422 | 42.2 | 138.6 |
| Airplane systems | 9 063 | 19 981 | 51.7 | 169.5 |
| Empty airplane | 133 063 | 293 353 | 67.0 | 219.7 |
| Passengers (234) | 17 513 | 38 610 | 42.1 | 138.2 |
| Cargo and containers | 4 844 | 10 680 | 55.6 | 182.5 |
| Crew | 720 | 1 585 | 34.2 | 112.1 |
| Services | 4 139 | 9 125 | 57.2 | 187.5 |
| Passengers, cargo and containers, crew, and services | 27 216 | 60 000 | 46.6 | 152.9 |
| Loaded airplane without fuel | 160 278 | 353 353 | 63.5 | 208.4 |

| 1. Report No. | 2. Government Accession No. | 3. Recipient's Catalog No. |
|---|---|---|
| NASA TN D-7218 | | |

| 4. Title and Subtitle | 5. Report Date |
|---|---|
| APPLICATION OF SONIC-BOOM MINIMIZATION CONCEPTS IN SUPERSONIC TRANSPORT DESIGN | June 1973 |
| | 6. Performing Organization Code |
| 7. Author(s) | 8. Performing Organization Report No. |
| Harry W. Carlson, Raymond L. Barger, and Robert J. Mack | L-8767 |
| | 10. Work Unit No. |
| 9. Performing Organization Name and Address | 501-06-11-01 |
| NASA Langley Research Center<br>Hampton, Va. 23665 | 11. Contract or Grant No. |
| | 13. Type of Report and Period Covered |
| 12. Sponsoring Agency Name and Address | Technical Note |
| National Aeronautics and Space Administration<br>Washington, D.C. 20546 | 14. Sponsoring Agency Code |

15. Supplementary Notes

16. Abstract

A study has been made of the applicability of sonic-boom minimization concepts in the design of large (234 passenger) supersonic transport airplanes capable of a 2500-nautical-mile range at a cruise Mach number of 2.7. Aerodynamics, weight and balance, and mission performance, as well as sonic-boom factors, have been taken into account. The results indicate that shock-strength nominal values of somewhat less than 48 newtons/meter$^2$ (1 pound force/foot$^2$) during cruise are within the realm of possibility. Because many of the design features are in direct contradiction to presently accepted design practices, further study by qualified airplane design teams is required to ascertain sonic-boom shock-strength levels actually attainable for practical supersonic transports.

| 17. Key Words (Suggested by Author(s)) | 18. Distribution Statement |
|---|---|
| Sonic-boom minimization<br>Airplane design | Unclassified – Unlimited |

| 19. Security Classif. (of this report) | 20. Security Classif. (of this page) | 21. No. of Pages | 22. Price* |
|---|---|---|---|
| Unclassified | Unclassified | 57 | $3.00 |

*For sale by the National Technical Information Service, Springfield, Virginia 22151